INTERNATIONAL CENTER FOR NUMERICAL METHODS IN ENGINEERING

Analysis of a Stabilized Finite Element Approximationof the Oseen Equations Using Orthogonal Subscale

R. Codina

Publication CIMNE Nº-289, May 2006

Analysis of a Stabilized Finite Element Approximationof the Oseen Equations Using Orthogonal Subscale

R. Codina

Publication CIMNE Nº-289, May 2006

International Center for Numerical Methods in Engineering
Gran Capitán s/n, 08034 Barcelona, Spain

Available online at www.sciencedirect.com
ScienceDirect
Applied Numerical Mathematics ••• (••••) •••–•••
APPLIED NUMERICAL MATHEMATICS
www.elsevier.com/locate/apnum

Analysis of a stabilized finite element approximation of the Oseen equations using orthogonal subscales

Ramon Codina

Universitat Politècnica de Catalunya, Jordi Girona 1-3, Edifici C1, 08034 Barcelona, Spain

Abstract

In this paper we present a stabilized finite element formulation to solve the Oseen equations as a model problem involving both convection effects and the incompressibility restriction. The need for stabilization techniques to solve this problem arises because of the restriction in the possible choices for the velocity and pressure spaces dictated by the inf–sup condition, as well as the instabilities encountered when convection is dominant. Both can be overcome by resorting from the standard Galerkin method to a stabilized formulation. The one presented here is based on the subgrid scale concept, in which unresolvable scales of the continuous solution are approximately accounted for. In particular, the approach developed herein is based on the assumption that unresolved subscales are orthogonal to the finite element space. It is shown that this formulation is stable and optimally convergent for an adequate choice of the algorithmic parameters on which the method depends.

Keywords: Convection-dominated flows; inf–sup condition; Stabilized finite element methods; Orthogonal subscales

1. Introduction

This paper deals with a finite element formulation to solve second-order boundary value problems with two main features: the presence of (dominant) first-order terms with the physical meaning of *convection* and the inclusion of constraints in the solution space, in our case *incompressibility*. The simplest linear model that contains *both* ingredients is the Oseen problem, which consists of finding a pair $[\boldsymbol{u}, p]$ as solution of the equations

$$-\nu\Delta\boldsymbol{u} + \boldsymbol{a}\cdot\nabla\boldsymbol{u} + \nabla p = \boldsymbol{f} \quad \text{in } \Omega \subset \mathbb{R}^d,\ d = 2, 3, \tag{1}$$

$$\nabla\cdot\boldsymbol{u} = 0 \quad \text{in } \Omega, \tag{2}$$

$$\boldsymbol{u} = \boldsymbol{0} \quad \text{on } \partial\Omega, \tag{3}$$

where $\boldsymbol{u}$ is the velocity field, p is the pressure, ν is the viscosity, $\boldsymbol{a}$ is the advection velocity, $\boldsymbol{f}$ is the vector of body forces, Ω is the computational domain, assumed to be bounded and polyhedral, and d is the number of space dimensions. For the sake of simplicity, we have considered the simplest Dirichlet condition (3). Likewise, several simplifying assumptions will be made for the advection velocity $\boldsymbol{a}$. In particular, we will take it in $\mathcal{C}^0(\bar{\Omega})$, weakly

E-mail address: ramon.codina@upc.edu (R. Codina).
URL: http://www.rmee.upc.es/homes/codina.

0168-9274/$30.00 © 2006 Published by Elsevier B.V. on behalf of IMACS.
doi:10.1016/j.apnum.2006.11.011

divergence free and with derivatives of order up to $k+1$ locally bounded by the maximum of $|\boldsymbol{a}|$ (see assumption H2 in Section 3.1).

The Oseen problem stated above can be thought of as a linearization of the stationary incompressible Navier–Stokes equations. It also appears as one of the steps of some multilevel methods for these equations, or may result from a time discretization of the transient Navier–Stokes problem if the advection velocity is treated explicitly. This is why it is often used as a first step towards the analysis of the full nonlinear problem, both to obtain *a priori* and *a posteriori* estimates.

Let us introduce some standard notation. The space of square integrable functions in a domain ω is denoted by $L^2(\omega)$, and the space of functions whose distributional derivatives of order up to $m \geqslant 0$ (integer) belong to $L^2(\omega)$ by $H^m(\omega)$. The space $H^1_0(\omega)$ consists of functions in $H^1(\omega)$ vanishing on $\partial\omega$. The topological dual of $H^1_0(\Omega)$ is denoted by $H^{-1}(\Omega)$, and the duality pairing by $\langle\cdot,\cdot\rangle$. A bold character is used to denote the vector counterpart of all these spaces. The L^2 inner product in ω (for scalars, vectors or tensors) is denoted by $(\cdot,\cdot)_\omega$, and the norm in a Banach space X by $\|\cdot\|_X$. This notation is simplified in some cases as follows: $(\cdot,\cdot)_\Omega \equiv (\cdot,\cdot)$, $\|\cdot\|_{L^2(\Omega)} \equiv \|\cdot\|$, for m integer (positive or negative) $\|\cdot\|_{H^m(\Omega)} \equiv \|\cdot\|_m$, and if K is the domain of an element (see below) $\|\cdot\|_{L^2(K)} \equiv \|\cdot\|_K$, $\|\cdot\|_{H^m(K)} \equiv \|\cdot\|_{m,K}$.

Using this notation, the velocity and pressure finite element spaces for the continuous problem are $\mathcal{V}_0 := \boldsymbol{H}^1_0(\Omega)$, $\mathcal{Q}_0 := L^2(\Omega)/\mathbb{R}$, $\mathcal{W}_0 := \mathcal{V}_0 \times \mathcal{Q}_0$. We shall be interested also in the larger spaces $\mathcal{V} := \boldsymbol{H}^1(\Omega)$, $\mathcal{Q} := L^2(\Omega)$, $\mathcal{W} := \mathcal{V} \times \mathcal{Q}$.

Let $\boldsymbol{U} \equiv [\boldsymbol{u}, p] \in \mathcal{W}_0$, $\boldsymbol{V} \equiv [\boldsymbol{v}, q] \in \mathcal{W}_0$. The variational statement for problem (1)–(2) can be written in terms of the bilinear form defined on $\mathcal{W}_0 \times \mathcal{W}_0$ as

$$B(\boldsymbol{U}, \boldsymbol{V}) := \nu(\nabla \boldsymbol{u}, \nabla \boldsymbol{v}) + (\boldsymbol{a} \cdot \nabla \boldsymbol{u}, \boldsymbol{v}) - (p, \nabla \cdot \boldsymbol{v}) + (q, \nabla \cdot \boldsymbol{u}). \tag{4}$$

Problem (1)–(2) with the homogeneous Dirichlet condition consists then in finding $\boldsymbol{U} \in \mathcal{W}_0$ such that

$$B(\boldsymbol{U}, \boldsymbol{V}) = \langle \boldsymbol{f}, \boldsymbol{v} \rangle =: L(\boldsymbol{V}), \quad \forall \boldsymbol{V} \in \mathcal{W}_0. \tag{5}$$

The standard Galerkin approximation of this abstract variational problem is now straightforward. Let $\mathcal{P}_h$ denote a finite element partition of the domain Ω. The diameter of an element domain $K \in \mathcal{P}_h$ is denoted by h_K and the diameter of the finite element partition by $h = \max\{h_K \mid K \in \mathcal{P}_h\}$. For simplicity, we assume that all the element domains are the image of a reference element $\hat{K}$ through a polynomial mapping, affine for simplicial elements, bilinear for quadrilaterals and trilinear for hexahedra. On $\hat{K}$ we define the polynomial spaces $R_k(\hat{K})$ where, as usual, $R_k = P_k$ for simplicial elements and $R_k = Q_k$ for quadrilaterals and hexahedra. From these polynomial spaces we can construct the conforming finite element spaces $\mathcal{V}_h \subset \mathcal{V}$ and $\mathcal{Q}_h \subset \mathcal{Q}$ in the usual manner, as well as the corresponding subspaces $\mathcal{V}_{h,0}$ and $\mathcal{Q}_{h,0}$. In principle, functions in $\mathcal{V}_h$ are continuous, whereas functions in $\mathcal{Q}_h$ not necessarily. Likewise, the orders k of these spaces may be different.

The discrete version of problem (5) is: find $\boldsymbol{U}_h \in \mathcal{W}_{h,0}$ such that

$$B(\boldsymbol{U}_h, \boldsymbol{V}_h) = L(\boldsymbol{V}_h), \quad \forall \boldsymbol{V}_h \in \mathcal{W}_{h,0}. \tag{6}$$

The well posedness of this problem relies on the ellipticity of the viscous term and the inf–sup or Babuška–Brezzi condition (see [7]), which can be shown to hold for the continuous problem. The first property is automatically inherited by its discrete counterpart. However, the inf–sup condition needs to be explicitly required. This leads to the need of using mixed interpolations, that is, different for $\boldsymbol{u}$ and p, and verifying

$$\inf_{q_h \in \mathcal{Q}_{h,0}} \sup_{\boldsymbol{v}_h \in \mathcal{V}_{h,0}} \frac{(q_h, \nabla \cdot \boldsymbol{v}_h)}{\|q_h\| \|\boldsymbol{v}_h\|_1} \geqslant \beta > 0, \tag{7}$$

for a constant β independent of h.

From the computational point of view, and also when Eq. (1) is generalized to include for example zero order terms in $\boldsymbol{u}$, it is convenient to use the same interpolation for the velocity and the pressure. This choice turns out to violate condition (7). This is why many of the so-called *stabilized* formulations have been proposed to approximate problem (5). The idea is to replace (6) by another discrete variational problem in which the bilinear form B is replaced by a possibly mesh dependent bilinear form B_h with enhanced stability properties. Examples of these type of methods are those of Brezzi and Pitkäranta [10], Brezzi and Douglas [6], Douglas and Wang [20], the Galerkin/least-squares

Please cite this article in press as: R. Codina, Analysis of a stabilized finite element approximation of the Oseen equations using orthogonal subscales, Applied Numerical Mathematics (2007), doi:10.1016/j.apnum.2006.11.011

(GLS) technique of Hughes et al. [28], Franca et al. [21,22] and first-order system least-squares methods (see e.g. [4] and references therein).

The second source of instability in the approximation of the Oseen equations arises because of the convective term. When it dominates the viscous one, the stability the latter provides is not enough to have control on the numerical solution and spurious oscillations may appear. Several strategies have been devised to overcome this problem, starting with the classical upwind discretizations. One of the most popular methods to stabilize convection in the finite element context is the so-called SUPG method [12]. Variants of this stabilization mechanism, which also allow to use equal velocity–pressure interpolation, can be found in [14,23,29,30].

In the next section, one of such stabilized formulations is described. It is based on the subgrid scale approach introduced by Hughes in [26,27] for the scalar convection–diffusion equation. The basic idea is to approximate the *effect* of the component of the continuous solution which cannot be resolved by the finite element mesh on the discrete finite element solution. An important feature of the formulation developed herein is that the unresolved subscales are assumed to be L^2 orthogonal to the finite element space. It turns out that for the Stokes problem (that it, when convection is absent) this method reduces to the one presented in [18], which was motivated by a completely different reasoning. After having stated two different variants of the proposed formulation, a complete numerical analysis of these is undertaken, showing its stability and convergence properties. Optimal *a priori* convergence estimates are proven for the h-version of the method. A third formulation, which is only intended to stabilize the pressure, is also analyzed. Two numerical examples are presented in Section 4 to show the good performance of the first of these formulations and finally some conclusions are drawn.

2. Description of the method

2.1. Algebraic subgrid scale methods

The finite element formulation to be analyzed in this paper has its roots in the so-called multiscale formulations of the problem [26,27]. The basic idea is to approximate the continuous space $\mathcal{W}$ by $\mathcal{W}_h \oplus \tilde{\mathcal{W}}$, where $\tilde{\mathcal{W}}$ is an approximation to the complement of $\mathcal{W}_h$ in $\mathcal{W}$. Likewise, $\mathcal{W}_0$ is approximated by $\mathcal{W}_{h,0} \oplus \tilde{\mathcal{W}}_0$, with $\tilde{\mathcal{W}}_0$ an approximation to the complement of $\mathcal{W}_{h,0}$ in $\mathcal{W}_0$. The space $\tilde{\mathcal{W}}_0$ will be called the space of *subgrid scales* or *subscales*. Assuming these are zero on the element boundaries, a possible way to construct $\tilde{\mathcal{W}}_0$ is by *bubble functions*. This leads to the *modified* discrete problem

$$B(\boldsymbol{U}_h, \boldsymbol{V}_h) + \sum_K \int_K \tilde{\boldsymbol{U}} \cdot \mathcal{L}^*(\boldsymbol{V}_h)\, \mathrm{d}\Omega = L(\boldsymbol{V}_h), \tag{8}$$

where $\sum_K$ stands for the summation over all $K \in \mathcal{P}_h$, $\mathcal{L}^*$ is the formal adjoint of the Oseen operator, which for divergence free advection velocities is given by

$$\mathcal{L}^*(\boldsymbol{V}_h) = \begin{bmatrix} -\nu \Delta \boldsymbol{v}_h - \boldsymbol{a} \cdot \nabla \boldsymbol{v}_h - \nabla q_h \\ -\nabla \cdot \boldsymbol{v}_h \end{bmatrix},$$

and $\tilde{\boldsymbol{U}}$ is the subscale to be approximated. Either the use of bubble functions or the approximation of the problem's Green function *suggest* to take $\tilde{\boldsymbol{U}}$ as [9]

$$\tilde{\boldsymbol{U}} = \boldsymbol{\tau}_K \big[\boldsymbol{F} - \mathcal{L}(\boldsymbol{U}_h) \big] \quad \text{in } K \in \mathcal{P}_h, \tag{9}$$

$\mathcal{L}$ being the Oseen operator and $\boldsymbol{\tau}_K$ a matrix of numerical parameters defined for each element domain $K \in \mathcal{P}_h$, which we will take as

$$\boldsymbol{\tau}_K = \mathrm{diag}(\boldsymbol{\tau}_{1,K}, \tau_{2,K}), \quad \boldsymbol{\tau}_{1,K} = \tau_{1,K} \boldsymbol{I}_d, \tag{10}$$

$$\tau_{1,K} = \left[\frac{c_1 \nu}{h^2_{K,\min}} + \frac{c_2 |\boldsymbol{a}|_{\infty,K}}{h_{K,\min}} \right]^{-1}, \tag{11}$$

$$\tau_{2,K} = c_3 \nu + c_4 |\boldsymbol{a}|_{\infty,K} h_{K,\min}, \tag{12}$$

where c_i are constants ($i = 1, 2, 3, 4$), on which precise conditions will be given later on, $\boldsymbol{I}_d$ is the $d \times d$ identity matrix, $|\boldsymbol{a}|_{\infty,K}$ is the maximum of the Euclidean norm of $\boldsymbol{a}$ in the element domain K and $h_{K,\min}$ is a function of

Please cite this article in press as: R. Codina, Analysis of a stabilized finite element approximation of the Oseen equations using orthogonal subscales, Applied Numerical Mathematics (2007), doi:10.1016/j.apnum.2006.11.011

the element diameter h_K which will be also precised later. The lack of analytical knowledge in the design of $\boldsymbol{\tau}_K$ will be substituted by the convergence analysis, which will establish whether this particular form is adequate or not. A heuristic justification of (9)–(12) based on a Fourier analysis of the problem of which $\tilde{\boldsymbol{U}}$ is solution can be found in [17].

At this point it is convenient to introduce some notation. For a set of symmetric and positive-definite matrices $\{\boldsymbol{\tau}_K,\ K \in \mathcal{P}_h\}$, we define the inner product weighted by these matrices and its associated norm by

$$(\boldsymbol{X}, \boldsymbol{Y})_\tau := \sum_K (\boldsymbol{\tau}_K \boldsymbol{X}, \boldsymbol{Y})_K, \quad \|\boldsymbol{Y}\|_\tau := \sqrt{(\boldsymbol{Y}, \boldsymbol{Y})_\tau}. \tag{13}$$

In these expressions, the functions $\boldsymbol{X}$ are $\boldsymbol{Y}$ need not being continuous for the local L^2 products to make sense. The inner product in (13) will play an essential role in the analysis of the following section. We may introduce also the inner products $(\cdot,\cdot)_{\tau_i}$, defined as in (13) using the elementwise value of the scalar algorithmic parameters τ_i $(i = 1, 2)$. This allows us to write problem (8) with the subscales approximated by (9) as

$$B_{\text{asgs}}(\boldsymbol{U}_h, \boldsymbol{V}_h) = L_{\text{asgs}}(\boldsymbol{V}_h) \quad \forall \boldsymbol{V}_h \in \mathcal{W}_0, \tag{14}$$

where

$$B_{\text{asgs}}(\boldsymbol{U}_h, \boldsymbol{V}_h) := B(\boldsymbol{U}_h, \boldsymbol{V}_h) + (-\nu\Delta\boldsymbol{u}_h + \boldsymbol{a}\cdot\nabla\boldsymbol{u}_h + \nabla p_h, \nu\Delta\boldsymbol{v}_h + \boldsymbol{a}\cdot\nabla\boldsymbol{v}_h + \nabla q_h)_{\tau_1} + (\nabla\cdot\boldsymbol{u}_h, \nabla\cdot\boldsymbol{v}_h)_{\tau_2}, \tag{15}$$

$$L_{\text{asgs}}(\boldsymbol{V}_h) := L(\boldsymbol{V}_h) + (\boldsymbol{f}, \nu\Delta\boldsymbol{v}_h + \boldsymbol{a}\cdot\nabla\boldsymbol{v}_h + \nabla q_h)_{\tau_1}. \tag{16}$$

A version of this method, including also zero order terms coming from Coriolis forces and permeability effects, is analyzed in [16].

2.2. Orthogonal subscales

It is shown in [15] that (9) can in fact be generalized to

$$\tilde{\boldsymbol{U}} = \boldsymbol{\tau}_K\big[\boldsymbol{F} - \mathcal{L}(\boldsymbol{U}_h)\big] + \boldsymbol{\tau}_K \boldsymbol{V}_{h,\text{ort}} \quad \text{in } K \in \mathcal{P}_h, \tag{17}$$

where $\boldsymbol{V}_{h,\text{ort}}$ is *any* element orthogonal to $\tilde{\mathcal{W}}_0$ (here and below, orthogonality is understood with respect to the L^2 inner product, unless otherwise specified).

Let us call Π_τ the projection onto $\mathcal{W}_h$ associated to the inner product in (13), hereafter referred to as τ*-projection*. Likewise, we will denote by $\Pi_{\tau,0}$ the τ-projection onto $\mathcal{W}_{h,0}$ and $\Pi_\tau^\perp := I - \Pi_\tau$, where I is the identity in $\mathcal{W}_h$. *If $\tilde{\mathcal{W}}$ is selected to be approximately orthogonal to $\mathcal{W}_h$, it can be shown that* [15]

$$\boldsymbol{V}_{h,\text{ort}} = -\Pi_\tau\big[\boldsymbol{F} - \mathcal{L}(\boldsymbol{U}_h)\big]. \tag{18}$$

The numerical formulation to be analyzed in this paper is obtained by using this in (17) and neglecting the orthogonal τ-projection of the viscous and force terms. The former are exactly zero for linear elements and for higher order interpolations disregarding them leads to a method which is still consistent (in a sense explained later; cf. Remark 3). The final *stabilized* formulation consists of finding $\boldsymbol{U}_h \in \mathcal{W}_0$ such that

$$B_I(\boldsymbol{U}_h, \boldsymbol{V}_h) = L(\boldsymbol{V}_h) \quad \forall \boldsymbol{V}_h \in \mathcal{W}_0, \tag{19}$$

where the bilinear form B_I is given by

$$B_I(\boldsymbol{U}_h, \boldsymbol{V}_h) = B(\boldsymbol{U}_h, \boldsymbol{V}_h) + \big(\Pi_{\tau_1}^\perp(\boldsymbol{a}\cdot\nabla\boldsymbol{u}_h + \nabla p_h), \boldsymbol{a}\cdot\nabla\boldsymbol{v}_h + \nabla q_h\big)_{\tau_1} + \big(\Pi_{\tau_2}^\perp(\nabla\cdot\boldsymbol{u}_h), \nabla\cdot\boldsymbol{v}_h\big)_{\tau_2}, \tag{20}$$

where B is defined in (4). Here and in what follows, the symbols Π_{τ_i}, $\Pi_{\tau_i,0}$ and $\Pi_{\tau_i}^\perp$ are used for the projections onto $\mathcal{V}_h$, $\mathcal{V}_{h,0}$ and $\mathcal{V}_h^\perp$, for $i = 1$, and onto $\mathcal{Q}_h$, $\mathcal{Q}_{h,0}$ and $\mathcal{Q}_h^\perp$, for $i = 2$. These projections are computed with the inner products $(\cdot,\cdot)_{\tau_i}$, $i = 1, 2$, respectively.

Once arrived to (20) it is observed that what the present method provides with respect to the standard Galerkin method is a *least-squares control on the component of the terms $\boldsymbol{a}\cdot\nabla\boldsymbol{u}_h + \nabla p_h$ and $\nabla\cdot\boldsymbol{u}_h$ orthogonal to the corresponding finite element spaces* with respect to the appropriate inner product. The objective of this paper is to analyze

Please cite this article in press as: R. Codina, Analysis of a stabilized finite element approximation of the Oseen equations using orthogonal subscales, Applied Numerical Mathematics (2007), doi:10.1016/j.apnum.2006.11.011

this formulation and to show that it is stable and optimally convergent. In spite of the fact that this analysis is different from that of the more classical method (14), mainly because B_I *will not be globally coercive*, we will obtain the same error estimates using different arguments. The differences in the implementation of (14) and (19) are discussed in Remark 2 below.

There is a simple modification of the bilinear form (20) which leads to another stabilized method with slightly better stability properties. The idea is to control separately the components of $\boldsymbol{a}\cdot\nabla\boldsymbol{u}_h$ and ∇p_h τ_1-orthogonal to $\mathcal{V}_h$. The bilinear form associated to this method is

$$B_{II}(\boldsymbol{U}_h,\boldsymbol{V}_h) = B(\boldsymbol{U}_h,\boldsymbol{V}_h) + \left(\Pi_{\tau_1}^{\perp}(\boldsymbol{a}\cdot\nabla\boldsymbol{u}_h),\boldsymbol{a}\cdot\nabla\boldsymbol{v}_h\right)_{\tau_1} + \left(\Pi_{\tau_1}^{\perp}(\nabla p_h),\nabla q_h\right)_{\tau_1} + \left(\Pi_{\tau_2}^{\perp}(\nabla\cdot\boldsymbol{u}_h),\nabla\cdot\boldsymbol{v}_h\right)_{\tau_2}. \tag{21}$$

Dropping the orthogonal projections $\Pi_{\tau_1}^{\perp}$ and $\Pi_{\tau_2}^{\perp}$, the method reduces to a general version of that analyzed in [14], which has a consistency error that makes it only applicable with P_1 elements. Likewise, when the convective term is absent the method coincides with that analyzed in [18] for the Stokes problem. In this situation, and when the meshes are made of patches of 2×2 quadrilaterals (in 2D), it is shown in [2] that the projections can be computed locally on each patch. Finally, let us mention the method proposed in [13] to stabilize convection which, like the stabilization of the convective term in (21), does not involve the whole residual of the equation to be solved.

Remark 1. Both methods I and II could be slightly modified by projecting onto $\mathcal{W}_{h,0}$ in (18) instead of projecting onto $\mathcal{W}_h$. This would simplify the analysis presented in the following section, since the stability condition (35) stated there would not be needed, and all the results to be presented carry over to this case. However, even though the global convergence is optimal, projecting onto $\mathcal{W}_{h,0}$ leads to spurious numerical boundary layers, similar to those found for the pressure in classical fractional step schemes for the transient problem (see for example [25]). Further discussion about this point can be found in [18].

2.3. Matrix form of the discrete problem

In order to highlight the modifications of the stabilized methods I and II (associated to the bilinear forms B_I and B_{II}, respectively) with respect to the standard Galerkin method, we consider here the matrix form of all these formulations.

The matrix form of the Galerkin method is

$$\begin{bmatrix} \mathsf{K}+\mathsf{A} & \mathsf{G} \\ \mathsf{D} & 0 \end{bmatrix}\begin{bmatrix} \mathsf{U} \\ \mathsf{P} \end{bmatrix} = \begin{bmatrix} \mathsf{F} \\ 0 \end{bmatrix},$$

where U and P are the arrays of nodal velocities and pressures, respectively, K is the matrix arising from the viscous term, A from the advection term, G from the pressure gradient, D from the velocity divergence and F is the resulting vector of nodal forces. Here and in the following we assume that the modifications on the first equation to account for the boundary conditions have *not yet* been performed.

Let us consider now method I, for simplicity with $\tau_{1,K}\equiv\tau_1$ constant for all the elements and $\tau_{2,K}=0$. The practical way to compute the orthogonal τ_1-projection $\Pi_{\tau_1}^{\perp}$ is to compute Π_{τ_1} and then use $\Pi_{\tau_1}^{\perp}=I-\Pi_{\tau_1}$. Therefore, if we call $\boldsymbol{\xi}_h$ the τ_1-projection of $\boldsymbol{a}\cdot\nabla\boldsymbol{u}_h+\nabla p_h$ onto $\mathcal{V}_h$ (which for τ_1 constant is equal to the L^2-projection) method I consists in fact of three discrete variational equations which allow to find $[\boldsymbol{u}_h,p_h,\boldsymbol{\xi}_h]\in\mathcal{V}_{h,0}\times\mathcal{Q}_{h,0}\times\mathcal{V}_h$, namely,

$$\begin{aligned}
&\nu(\nabla\boldsymbol{u}_h,\nabla\boldsymbol{v}_h)+(\boldsymbol{a}\cdot\nabla\boldsymbol{u}_h,\boldsymbol{v}_h)+(\nabla p_h,\boldsymbol{v}_h)+\tau_1(\boldsymbol{a}\cdot\nabla\boldsymbol{u}_h+\nabla p_h-\boldsymbol{\xi}_h,\boldsymbol{a}\cdot\nabla\boldsymbol{v}_h)=\langle\boldsymbol{f},\boldsymbol{v}_h\rangle,\\
&(q_h,\nabla\cdot\boldsymbol{u}_h)+\tau_1(\nabla q_h,\boldsymbol{a}\cdot\nabla\boldsymbol{u}_h+\nabla p_h-\boldsymbol{\xi}_h)=0,\\
&(\boldsymbol{a}\cdot\nabla\boldsymbol{u}_h+\nabla p_h,\boldsymbol{\eta}_h)-(\boldsymbol{\xi}_h,\boldsymbol{\eta}_h)=0,
\end{aligned}$$

which must hold for all $[\boldsymbol{v}_h,q_h,\boldsymbol{\eta}_h]\in\mathcal{V}_{h,0}\times\mathcal{Q}_{h,0}\times\mathcal{V}_h$. If we denote by a subscript a the matrices arising from terms weighted by $\boldsymbol{a}\cdot\nabla\boldsymbol{v}_h$ (which suggests 'derivative with respect to $\boldsymbol{a}$') and by subscript d the matrices arising from terms weighted by $-\nabla q_h$ (suggesting the 'divergence'), it is easy to see that the matrix version of the previous equations is

$$\begin{bmatrix} \mathsf{K}+\mathsf{A}+\tau_1\mathsf{A}_a & \mathsf{G}+\tau_1\mathsf{G}_a & -\tau_1\mathsf{M}_a \\ \mathsf{D}-\tau_1\mathsf{A}_d & -\tau_1\mathsf{G}_d & \tau_1\mathsf{M}_d \\ \mathsf{A} & \mathsf{G} & -\mathsf{M} \end{bmatrix}\begin{bmatrix} \mathsf{U} \\ \mathsf{P} \\ \Xi \end{bmatrix} = \begin{bmatrix} \mathsf{F} \\ 0 \\ 0 \end{bmatrix}, \tag{22}$$

Please cite this article in press as: R. Codina, Analysis of a stabilized finite element approximation of the Oseen equations using orthogonal subscales, Applied Numerical Mathematics (2007), doi:10.1016/j.apnum.2006.11.011

where M is the Gramm matrix of the finite element interpolation, and thus M_a and M_d the matrices obtained by replacing the test function $\boldsymbol{\eta}_h$ by $\boldsymbol{a}\cdot\nabla\boldsymbol{v}_h$ and $-\nabla q_h$, respectively.

The algebraic problem (22) can be solved using a block iteration algorithm segregating the calculation of Ξ from that of U and P. However, if an iterative solver is used, it is also feasible to solve it in a direct monolithic way. The array Ξ can be formally condensed to yield the system

$$\begin{bmatrix} \mathsf{K}+\mathsf{A}+\tau_1(\mathsf{A}_a-\mathsf{M}_a\mathsf{M}^{-1}\mathsf{A}) & \mathsf{G}+\tau_1(\mathsf{G}_a-\mathsf{M}_a\mathsf{M}^{-1}\mathsf{G}) \\ \mathsf{D}+\tau_1(\mathsf{M}_d\mathsf{M}^{-1}\mathsf{A}-\mathsf{A}_d) & \tau_1(\mathsf{M}_d\mathsf{M}^{-1}\mathsf{G}-\mathsf{G}_d) \end{bmatrix} \begin{bmatrix} \mathsf{U} \\ \mathsf{P} \end{bmatrix} = \begin{bmatrix} \mathsf{F} \\ 0 \end{bmatrix}. \tag{23}$$

Iterative solvers for this system only require the evaluation of matrix–vector products. The only point to be considered when solving (23) is the evaluation of $\mathsf{M}^{-1}\mathsf{Z}=\mathsf{Y}$ for a given array Z, which implies solving the system $\mathsf{Z}=\mathsf{MY}$. This can be done very efficiently using Jacobi iterations and taking as preconditioner a diagonal approximation to M. Usually, two or three iterations are sufficient, and their computational cost in the overall calculation is negligible. This is the approach we have followed in the numerical examples.

Let us consider now method II, which consists of finding $[\boldsymbol{u}_h, p_h, \boldsymbol{\xi}_{h,1}, \boldsymbol{\xi}_{h,2}] \in \mathcal{V}_{h,0}\times\mathcal{Q}_{h,0}\times\mathcal{V}_h\times\mathcal{V}_h$ such that

$$\begin{aligned}
&\nu(\nabla\boldsymbol{u}_h,\nabla\boldsymbol{v}_h)+(\boldsymbol{a}\cdot\nabla\boldsymbol{u}_h,\boldsymbol{v}_h)+(\nabla p_h,\boldsymbol{v}_h)+\tau_1(\boldsymbol{a}\cdot\nabla\boldsymbol{u}_h-\boldsymbol{\xi}_{h,1},\boldsymbol{a}\cdot\nabla\boldsymbol{v}_h)=\langle\boldsymbol{f},\boldsymbol{v}_h\rangle,\\
&(q_h,\nabla\cdot\boldsymbol{u}_h)+\tau_1(\nabla q_h,\nabla p_h-\boldsymbol{\xi}_{h,2})=0,\\
&(\boldsymbol{a}\cdot\nabla\boldsymbol{u}_h,\boldsymbol{\eta}_{h,1})-(\boldsymbol{\xi}_{h,1},\boldsymbol{\eta}_{h,1})=0,\\
&(\nabla p_h,\boldsymbol{\eta}_{h,2})-(\boldsymbol{\xi}_{h,2},\boldsymbol{\eta}_{h,2})=0,
\end{aligned}$$

for all $[\boldsymbol{v}_h, q_h, \boldsymbol{\eta}_{h,1}, \boldsymbol{\eta}_{h,2}] \in \mathcal{V}_{h,0}\times\mathcal{Q}_{h,0}\times\mathcal{V}_h\times\mathcal{V}_h$. The matrix version of this discrete variational problem is

$$\begin{bmatrix} \mathsf{K}+\mathsf{A}+\tau_1\mathsf{A}_a & \mathsf{G} & -\tau_1\mathsf{M}_a & 0 \\ \mathsf{D} & -\tau_1\mathsf{G}_d & 0 & \tau_1\mathsf{M}_d \\ \mathsf{A} & 0 & -\mathsf{M} & 0 \\ 0 & \mathsf{G} & 0 & -\mathsf{M} \end{bmatrix} \begin{bmatrix} \mathsf{U} \\ \mathsf{P} \\ \Xi_1 \\ \Xi_2 \end{bmatrix} = \begin{bmatrix} \mathsf{F} \\ 0 \\ 0 \\ 0 \end{bmatrix}, \tag{24}$$

and the condensed counterpart is

$$\begin{bmatrix} \mathsf{K}+\mathsf{A}+\tau_1(\mathsf{A}_a-\mathsf{M}_a\mathsf{M}^{-1}\mathsf{A}) & \mathsf{G} \\ \mathsf{D} & \tau_1(\mathsf{M}_d\mathsf{M}^{-1}\mathsf{G}-\mathsf{G}_d) \end{bmatrix} \begin{bmatrix} \mathsf{U} \\ \mathsf{P} \end{bmatrix} = \begin{bmatrix} \mathsf{F} \\ 0 \end{bmatrix}. \tag{25}$$

The difference in the terms introduced by methods I and II is clearly observed by comparing (22) and (24) or (23) and (25). It is seen that method II introduces less terms, but two projections onto $\mathcal{V}_h$ need to be performed.

Remark 2. After having described the algebraic problem obtained from the stabilization with orthogonal subscales, it is important to mention the differences with the more usual method (14), which is similar to the classical SUPG or GLS methods. First of all, in these cases the *whole* element residual needs to be computed within each element. In particular, second-order derivatives of the shape functions have to be computed and stored for higher order elements, a cumbersome and time consuming process. Likewise, the right-hand side of the algebraic system needs to be modified. The advantage with respect to method (19) analyzed here is that no variables other than the velocity and the pressure need to be dealt with. In particular, no projections need to be performed. The relative importance of these two facts depends on the numerical example being solved.

3. Numerical analysis

3.1. Preliminaries

In this section we prove that methods I and II are stable and optimally convergent. We will consider also a slight modification of these methods that is only intended to stabilize the pressure, and therefore with poor stability properties for convection dominated flows. However, this method allows us to prove convergence in a finer norm than for methods I and II.

Please cite this article in press as: R. Codina, Analysis of a stabilized finite element approximation of the Oseen equations using orthogonal subscales, Applied Numerical Mathematics (2007), doi:10.1016/j.apnum.2006.11.011

Let us state now some properties of the family of finite element partitions $\mathcal{F} := \{\mathcal{P}_h \mid h > 0\}$ that we will use. First, we assume that $\mathcal{F}$ is nondegenerate (that is, the quotient h_K/ϱ_K remains bounded, with ϱ_K the diameter of the ball inscribed in K), and therefore the inverse estimate

$$\|\nabla v_h\|_K \leqslant \frac{C_{\text{inv}}}{h_K}\|v_h\|_K, \quad K \in \mathcal{P}_h, \tag{26}$$

holds for any finite element function v_h (see, e.g., [5]).

The precise conditions we will need for the constants c_i in (11) and (12) can be written in terms of the constant C_{inv} in the inverse estimate (26). Although other choices for these conditions are possible, we will assume that

$$c_1 = \alpha^2 C_{\text{inv}}^2, \quad c_2 = \alpha C_{\text{inv}}, \quad \text{with } \alpha > 1, \tag{27}$$

$$c_3 = \sigma, \quad c_4 = \frac{\sigma}{\alpha C_{\text{inv}}}, \quad \text{with } 0 < \sigma \leqslant 1. \tag{28}$$

We shall restrict our attention to interpolations of degree k *for both the velocity and the pressure*, although the extension to different velocity–pressure interpolations offers no difficulty, *provided the pressure interpolation is continuous*.

We will need the following approximation property: for any function v in $H^r(\Omega)$, $0 \leqslant r \leqslant k+1$, there exists a finite element interpolant $\hat{v}_h$ such that

$$\|v - \hat{v}_h\|_{m,K} \leqslant C_I h_K^{n-m}\|v\|_{H^n(S_K)}, \quad 0 \leqslant n \leqslant r,\ 0 \leqslant m \leqslant n,$$

for $K \in \mathcal{P}_h$, where C_I is a positive constant and S_K is the patch of elements neighboring K and $m,\ n,\ r$ are integers [5]. For $n \geqslant 2$ and $d = 2, 3$, $\hat{v}_h$ can be taken as the standard nodal interpolant and S_K can be replaced by K.

For nondegenerate $\mathcal{F}$ the patches are quasi-uniform, that is, there exist positive constants C and C' such that (cf. [1, Theorem 1.9]):

$$Ch_{K'} \leqslant h_K \leqslant C'h_{K'}, \quad \forall K' \in S_K,\ \forall K \in \mathcal{P}_h, \tag{29}$$

which allows us to write the interpolation estimate as

$$\|v - \hat{v}_h\|_{m,K} \leqslant C_I \sum_{K' \subset S_K} h_{K'}^{n-m}\|v\|_{n,K'}, \quad 0 \leqslant n \leqslant r,\ 0 \leqslant m \leqslant n, \tag{30}$$

for $K \in \mathcal{P}_h$. Likewise, (29) is the basic ingredient to prove the following property of the family $\mathcal{F}$:

Lemma 1. *Let $\boldsymbol{x}_K$ be the coordinates of the barycenter of an element domain K. If the family of finite element partitions $\mathcal{F}$ is nondegenerate, then there exist functions χ_1, χ_2, with $\chi_1(\cdot, h), \chi_2(\cdot, h) \in \mathcal{C}^0(\Omega)$ for all $h > 0$, such that*

$$h_{K,\min} := \chi_1(\boldsymbol{x}_K, h) \leqslant h_K \leqslant \chi_2(\boldsymbol{x}_K, h), \quad \forall K \in \mathcal{P}_h,\ h > 0,$$

$$\sup_{h>0}\sup_{\boldsymbol{x}\in\Omega}\frac{\chi_2(\boldsymbol{x}, h)}{\chi_1(\boldsymbol{x}, h)} \leqslant \chi_0 < \infty.$$

Proof. Let a be a vertex node of the finite element partition and let h_a be the average of the element diameters of the elements to which a belongs. If $H(\boldsymbol{x}, h)$ is the piecewise continuous interpolation of degree one from the nodal values h_a, (29) implies that

$$A_1 H(\boldsymbol{x}_K, h) \leqslant h_K \leqslant A_2 H(\boldsymbol{x}_K, h)$$

for constants $A_1,\ A_2 > 0$. The result follows taking $\chi_i(\boldsymbol{x}, h) = A_i H(\boldsymbol{x}, h)$, $i = 1, 2$ (and $\chi_0 = A_2/A_1$). □

Observe that $h_{K,\min}$ appears in the definition of the stabilization parameters (11) and (12) (other choices are also possible by modifying conditions (27) and (28)). From the continuity of $\boldsymbol{a}$ and (29), these parameters will satisfy

$$C\tau_{i,K'} \leqslant \tau_{i,K} \leqslant C'\tau_{i,K'}, \quad \forall K' \in S_K,\ \forall K \in \mathcal{P}_h,\ i = 1, 2, \tag{31}$$

Please cite this article in press as: R. Codina, Analysis of a stabilized finite element approximation of the Oseen equations using orthogonal subscales, Applied Numerical Mathematics (2007), doi:10.1016/j.apnum.2006.11.011

for constants $C,\ C' > 0$, not necessarily the same as before. In what follows, C denotes a positive constant, independent of the mesh size h and of the coefficients of the differential equation. The value of C may vary in its different appearances.

Lemma 1 allows us to make the following construction. For each $h > 0$, let $\mathcal{N}_h$ be the set of nodal points of the partition $\mathcal{P}_h$. Scalar continuous finite element functions are uniquely determined by their values at the nodes in $\mathcal{N}_h$. Likewise, we denote by $\mathcal{N}_K$ the set of nodes in an element domain $K \in \mathcal{P}_h$. If a is a node, with coordinates $\boldsymbol{x}_a$, we may now construct a set of algorithmic parameters $\{\bar{\tau}_{i,a} \mid a \in \mathcal{N}_h,\ i = 1, 2\}$, where $\tau_{i,a}$ is simply defined by replacing in (11)–(12) the element parameter $h_{K,\min}$ by $\chi_1(\boldsymbol{x}_a, h)$ and $|\boldsymbol{a}|_{\infty,K}$ by the Euclidean norm of $\boldsymbol{a}$ evaluated at $\boldsymbol{x}_a$.

To prove stability (cf. Theorems 1, 3, 5), we will need in particular to take the velocity test function close to $\tau_{1,K}\Pi_{\tau_1,0}(\boldsymbol{\xi}_h)$ within each element domain K (for certain $\boldsymbol{\xi}_h$). Unfortunately, these functions are discontinuous, and therefore we will need to approximate them by continuous functions, belonging to the finite element space. We construct these approximations as follows. Let $N_a(\boldsymbol{x}),\ \boldsymbol{x} \in \Omega$, be the standard shape (basis) function associated to node $a \in \mathcal{N}_h$. A finite element function v_h can be thus written as

$$v_h(\boldsymbol{x})|_K = \sum_{a \in \mathcal{N}_K} N_a(\boldsymbol{x})|_K v^a, \quad K \in \mathcal{P}_h,$$

where $\{v^a \mid a \in \mathcal{N}_K\}$ is the set of element nodal parameters of v_h. From $\{\bar{\tau}_{i,a} \mid a \in \mathcal{N}_h,\ i = 1, 2\}$ and $\{\tau_{i,K} \mid K \in \mathcal{P}_h,\ i = 1, 2\}$ we define

$$\tau \circ v_h \quad \text{by } \tau \circ v_h(\boldsymbol{x})|_K := \tau_K v_h(\boldsymbol{x})|_K, \tag{32}$$

$$\tau \diamond v_h \quad \text{by } \tau \diamond v_h(\boldsymbol{x})|_K := \sum_{a \in \mathcal{N}_K} N_a(\boldsymbol{x})|_K \bar{\tau}_a v^a. \tag{33}$$

Here and in the following result τ may be either τ_1 or τ_2:

Lemma 2. *Assume that the family $\mathcal{F}$ of finite element partitions is nondegenerate. Then, for any finite element function v_h, the functions $\tau \circ v_h$ and $\tau \diamond v_h$ defined in* (32) *and* (33)*, respectively, satisfy*

$$\|\tau \circ v_h - \tau \diamond v_h\|_K \leqslant \tau_K \psi(h) \|v_h\|_K, \tag{34}$$

where $\psi(h) \to 0$ as $h \to 0$.

Proof. For any piecewise continuous finite element function w_h we have that

$$C_1 h_K^{d/2} \|w_h\|_{L^\infty(K)} \leqslant \|w_h\|_{L^2(K)} \leqslant C_2 h_K^{d/2} \|w_h\|_{L^\infty(K)},$$

where C_1 and C_2 are positive constants. The first inequality is an inverse estimate valid for nondegenerate $\mathcal{F}$ (see [5]) and the second is obvious. Using this we obtain

$$\begin{aligned}
C_2^{-1} h_K^{-d/2} \|\tau \circ v_h - \tau \diamond v_h\|_{L^2(K)} &\leqslant \|\tau \circ v_h - \tau \diamond v_h\|_{L^\infty(K)} \\
&= \left\| \sum_{a \in \mathcal{N}_K} (\tau_K - \bar{\tau}_a) N_a(\boldsymbol{x}) v^a \right\|_{L^\infty(K)} \\
&\leqslant \tau_K \max_{a \in \mathcal{N}_K} \left| \frac{\bar{\tau}_a}{\tau_K} - 1 \right| \left\| \sum_{a \in \mathcal{N}_K} |N_a(\boldsymbol{x}) v^a| \right\|_{L^\infty(K)} \\
&\leqslant C \tau_K \max_{a \in \mathcal{N}_K} \left| \frac{\bar{\tau}_a}{\tau_K} - 1 \right| \|v_h\|_{L^\infty(K)} \\
&\leqslant C \tau_K \max_{a \in \mathcal{N}_K} \left| \frac{\bar{\tau}_a}{\tau_K} - 1 \right| C_1^{-1} h_K^{-d/2} \|v_h\|_{L^2(K)},
\end{aligned}$$

for a positive constant C. From the continuity assumed for the advection velocity $\boldsymbol{a}$ we have that $\bar{\tau}_a \to \tau_K$ as $h \to 0$, and the result follows. □

This result and definitions (32) and (33) are also valid when v_h is a vector function. We have thus constructed a continuous function $\tau \diamond v_h$ that approximates $\tau \circ v_h$ when the mesh diameter goes to zero.

Please cite this article in press as: R. Codina, Analysis of a stabilized finite element approximation of the Oseen equations using orthogonal subscales, Applied Numerical Mathematics (2007), doi:10.1016/j.apnum.2006.11.011

The final assumption is that we will assume that there is a constant $\beta_0 > 0$ such that

$$\|z_h\|_{\tau_1} \leqslant \frac{1}{\beta_0} \left\| \Pi_{\tau_1,0}(z_h) + \Pi_{\tau_1}^{\perp}(z_h) \right\|_{\tau_1}, \quad z_h \equiv \boldsymbol{a} \cdot \nabla \boldsymbol{v}_h + \nabla q_h, \tag{35}$$

for all $[\boldsymbol{v}_h, q_h] \in \mathcal{V}_{h,0} \times \mathcal{Q}_{h,0}$ and for $h > 0$. This condition means that a bound for the norms of $\Pi_{\tau_1,0}(z_h)$ and $\Pi_{\tau_1}^{\perp}(z_h)$ is enough to bound the whole norm of vector z_h, which in turn implies that the component of z_h in $\mathcal{V}_h$ which is τ_1-orthogonal to $\mathcal{V}_{h,0}$ is not independent of the other two components, $\Pi_{\tau_1,0}(z_h)$ and $\Pi_{\tau_1}^{\perp}(z_h)$.

We will not pursue a study of this condition in this paper. The assumption that it holds will be one of the hypothesis of the analysis presented below. Let us only mention that exactly the same analysis as in [18] can be applied here, and can be used to prove that it holds for example in the case of P_k elements. Nevertheless, we insist on the fact that this condition is not essential, in the sense explained in Remark 1.

For $z_h = \nabla \cdot \boldsymbol{v}_h$ (now a scalar), and replacing $\tau_{1,K}$ by $\tau_{2,K}$, it is trivially verified that (35) always holds with $\beta_0 = 1$, since $\boldsymbol{v}_h = \boldsymbol{0}$ on $\partial\Omega$ implies that $\nabla \cdot \boldsymbol{v}_h$ has zero mean, and therefore $\Pi_{\tau_2,0}(\nabla \cdot \boldsymbol{v}_h) = \Pi_{\tau_2}(\nabla \cdot \boldsymbol{v}_h)$. However, to keep the notation compact, we will use also (35) in this case.

The stability condition (35) completes the set of assumptions that will be used in the following. For future reference, let us collect them:

H1. The advection velocity $\boldsymbol{a}$ is in $\mathcal{C}^0(\bar{\Omega})$ and weakly divergence free.
H2. There is a constant C_D such that the $k+1$ derivatives of $\boldsymbol{a}$ within element K are bounded above by $C_D|\boldsymbol{a}|_{\infty,K}$, $K \in \mathcal{P}_h$.
H3. The family $\mathcal{F}$ of finite element partitions is nondegenerate.
H4. The stability condition (35) holds.
H5. The algorithmic parameters $\tau_{1,K}$ and $\tau_{2,K}$ are given by (11) and (12), respectively, with the constants c_i given by (27)–(28).
H6. The data are such that the exact velocity components are in $H^{k+1}(\Omega)$ and the exact pressure in $H^k(\Omega)$, $k \geqslant 1$.

Assumption H6 will only be needed to prove that convergence is optimal when finite element interpolations of degree k are used. We will call

$$\varepsilon(h) := \sum_K \left(\tau_{1,K}^{-1/2} h_K^{k+1} \|\boldsymbol{u}\|_{k+1,K} + \tau_{2,K}^{-1/2} h_K^k \|p\|_{k,K} \right). \tag{36}$$

The ultimate purpose of the analysis below is to show that this is the error function (in norms to be defined) of the different methods considered.

3.2. Method I

The problem in this case is stated in (19). We prove now that this method is stable and convergent in the mesh dependent norm

$$|||\boldsymbol{V}_h|||_I \equiv \left|||[\boldsymbol{v}_h, q_h]|||_I := \nu^{1/2} \|\nabla \boldsymbol{v}_h\| + \|\boldsymbol{a} \cdot \nabla \boldsymbol{v}_h + \nabla q_h\|_{\tau_1} + \|\nabla \cdot \boldsymbol{v}_h\|_{\tau_2}. \tag{37}$$

Theorem 1 *(Stability of method I). Under assumptions* H1, H3, H4 *and* H5*, there is a constant $\beta_I > 0$ such that, for h sufficiently small and α in* (27)–(28) *large enough,*

$$\inf_{\boldsymbol{U}_h \in \mathcal{W}_{h,0}} \sup_{\boldsymbol{V}_h \in \mathcal{W}_{h,0}} \frac{B_I(\boldsymbol{U}_h, \boldsymbol{V}_h)}{|||\boldsymbol{U}_h|||_I |||\boldsymbol{V}_h|||_I} \geqslant \beta_I. \tag{38}$$

Proof. Fix $\boldsymbol{U}_h \equiv [\boldsymbol{u}_h, p_h] \in \mathcal{W}_{h,0}$, arbitrary, and let us introduce the abbreviations $\boldsymbol{\xi}_h \equiv \boldsymbol{a} \cdot \nabla \boldsymbol{u}_h + \nabla p_h$, $\delta_h \equiv \nabla \cdot \boldsymbol{u}_h$. From the definition of B_I it follows that

$$B_I\big([\boldsymbol{u}_h, p_h], [\boldsymbol{u}_h, p_h]\big) = \nu \|\nabla \boldsymbol{u}_h\|^2 + \left\|\Pi_{\tau_1}^{\perp}(\boldsymbol{\xi}_h)\right\|_{\tau_1}^2 + \left\|\Pi_{\tau_2}^{\perp}(\delta_h)\right\|_{\tau_2}^2. \tag{39}$$

Clearly, B_I is not coercive in the norm (37). All we can expect is stability in the form given by (38). If now we take $[\boldsymbol{v}_h, q_h] = [\tau_1 \diamond \Pi_{\tau_1,0}(\boldsymbol{\xi}_h), \tau_2 \diamond \Pi_{\tau_2,0}(\delta_h)]$ it is found that

Please cite this article in press as: R. Codina, Analysis of a stabilized finite element approximation of the Oseen equations using orthogonal subscales, Applied Numerical Mathematics (2007), doi:10.1016/j.apnum.2006.11.011

$$
\begin{aligned}
&B_I\big([\boldsymbol{u}_h, p_h], \big[\tau_1 \diamond \Pi_{\tau_1,0}(\boldsymbol{\xi}_h), \tau_2 \diamond \Pi_{\tau_2,0}(\delta_h)\big]\big)\\
&\quad = \nu\big(\nabla \boldsymbol{u}_h, \nabla\big[\tau_1 \diamond \Pi_{\tau_1,0}(\boldsymbol{\xi}_h)\big]\big) + \big(\boldsymbol{\xi}_h, \tau_1 \circ \Pi_{\tau_1,0}(\boldsymbol{\xi}_h)\big) + \big(\boldsymbol{\xi}_h, \tau_1 \diamond \Pi_{\tau_1,0}(\boldsymbol{\xi}_h) - \tau_1 \circ \Pi_{\tau_1,0}(\boldsymbol{\xi}_h)\big)\\
&\qquad + \big(\tau_2 \circ \Pi_{\tau_2,0}(\delta_h), \delta_h\big) + \big(\tau_2 \diamond \Pi_{\tau_2,0}(\delta_h) - \tau_2 \circ \Pi_{\tau_2,0}(\delta_h), \delta_h\big)\\
&\qquad + \big(\boldsymbol{a} \cdot \nabla\big[\tau_1 \diamond \Pi_{\tau_1,0}(\boldsymbol{\xi}_h)\big], \Pi^{\perp}_{\tau_1}(\boldsymbol{\xi}_h)\big)_{\tau_1} + \big(\nabla\big[\tau_2 \diamond \Pi_{\tau_2,0}(\delta_h)\big], \Pi^{\perp}_{\tau_1}(\boldsymbol{\xi}_h)\big)_{\tau_1}\\
&\qquad + \big(\nabla \cdot \big[\tau_1 \diamond \Pi_{\tau_1,0}(\boldsymbol{\xi}_h)\big], \Pi^{\perp}_{\tau_2}(\delta_h)\big)_{\tau_2}. \qquad (40)
\end{aligned}
$$

Note that

$$
\big(\boldsymbol{\xi}_h, \tau_1 \circ \Pi_{\tau_1,0}(\boldsymbol{\xi}_h)\big) = \big(\boldsymbol{\xi}_h, \Pi_{\tau_1,0}(\boldsymbol{\xi}_h)\big)_{\tau_1} = \big\|\Pi_{\tau_1,0}(\boldsymbol{\xi}_h)\big\|^2_{\tau_1},
$$

and, similarly, $(\tau_2 \circ \Pi_{\tau_2,0}(\delta_h), \delta_h) = \|\Pi_{\tau_2,0}(\delta_h)\|^2_{\tau_2}$. This, Schwarz's inequality and the inverse estimate (26) in (40) imply

$$
\begin{aligned}
&B_I\big([\boldsymbol{u}_h, p_h], \big[\tau_1 \diamond \Pi_{\tau_1,0}(\boldsymbol{\xi}_h), \tau_2 \diamond \Pi_{\tau_2,0}(\delta_h)\big]\big)\\
&\quad \geqslant -\sum_K \frac{C_{\mathrm{inv}}}{h_K} \nu \|\nabla \boldsymbol{u}_h\|_K \big\|\tau_1 \diamond \Pi_{\tau_1,0}(\boldsymbol{\xi}_h)\big\|_K\\
&\qquad + \big\|\Pi_{\tau_1,0}(\boldsymbol{\xi}_h)\big\|^2_{\tau_1} - \sum_K \|\boldsymbol{\xi}_h\|_K \big\|\tau_1 \diamond \Pi_{\tau_1,0}(\boldsymbol{\xi}_h) - \tau_1 \circ \Pi_{\tau_1,0}(\boldsymbol{\xi}_h)\big\|_K\\
&\qquad + \big\|\Pi_{\tau_2,0}(\delta_h)\big\|^2_{\tau_2} - \sum_K \|\delta_h\|_K \big\|\tau_2 \diamond \Pi_{\tau_2,0}(\delta_h) - \tau_2 \circ \Pi_{\tau_2,0}(\delta_h)\big\|_K\\
&\qquad - \sum_K \frac{C_{\mathrm{inv}}}{h_K} |\boldsymbol{a}|_{\infty,K} \tau_{1,K} \big\|\tau_1 \diamond \Pi_{\tau_1,0}(\boldsymbol{\xi}_h)\big\|_K \big\|\Pi^{\perp}_{\tau_1}(\boldsymbol{\xi}_h)\big\|_K - \sum_K \frac{C_{\mathrm{inv}}}{h_K} \tau_{1,K} \big\|\tau_2 \diamond \Pi_{\tau_2,0}(\delta_h)\big\|_K \big\|\Pi^{\perp}_{\tau_1}(\boldsymbol{\xi}_h)\big\|_K\\
&\qquad - \sum_K \frac{C_{\mathrm{inv}}}{h_K} \tau_{2,K} \big\|\tau_1 \diamond \Pi_{\tau_1,0}(\boldsymbol{\xi}_h)\big\|_K \big\|\Pi^{\perp}_{\tau_2}(\delta_h)\big\|_K. \qquad (41)
\end{aligned}
$$

The bounds (27)–(28) assumed for the constants c_i in the definition of $\tau_{1,K}$ and $\tau_{2,K}$ imply

$$
\frac{C_{\mathrm{inv}}}{h_K} \nu^{1/2} \leqslant \frac{1}{\alpha} \tau_{1,K}^{-1/2}, \qquad \frac{C_{\mathrm{inv}}}{h_K} |\boldsymbol{a}|_{\infty,K} \leqslant \frac{1}{\alpha} \tau_{1,K}^{-1}, \qquad \frac{C_{\mathrm{inv}}}{h_K} \tau_{1,K}^{1/2} \tau_{2,K}^{1/2} \leqslant \frac{1}{\alpha}.
$$

Using these inequalities, Lemma 2 (which implies that $\|\tau \diamond v_h\| \leqslant \tau_K (1 + \psi(h)) \|v_h\|_K$), and the arithmetic–geometric inequality, it can be readily verified that

$$
\begin{aligned}
&B_I\big([\boldsymbol{u}_h, p_h], \big[\tau_1 \diamond \Pi_{\tau_1,0}(\boldsymbol{\xi}_h), \tau_2 \diamond \Pi_{\tau_2,0}(\delta_h)\big]\big)\\
&\quad \geqslant -\frac{1}{2\alpha}\big[1 + \psi(h)\big] \nu \|\nabla \boldsymbol{u}_h\|^2 + \left[1 - \frac{3}{2\alpha}\big[1 + \psi(h)\big] - \frac{1}{2}\psi(h)\right] \big\|\Pi_{\tau_1,0}(\boldsymbol{\xi}_h)\big\|^2_{\tau_1}\\
&\qquad - \frac{1}{\alpha}\big[1 + \psi(h)\big] \big\|\Pi^{\perp}_{\tau_1}(\boldsymbol{\xi}_h)\big\|^2_{\tau_1} - \frac{1}{2}\psi(h) \|\boldsymbol{\xi}_h\|^2_{\tau_1} + \left[1 - \frac{1}{2\alpha}\big[1 + \psi(h)\big] - \frac{1}{2}\psi(h)\right] \big\|\Pi_{\tau_2,0}(\delta_h)\big\|^2_{\tau_2}\\
&\qquad - \frac{1}{2\alpha}\big[1 + \psi(h)\big] \big\|\Pi^{\perp}_{\tau_2}(\delta_h)\big\|^2_{\tau_1} - \frac{1}{2}\psi(h) \|\delta_h\|^2_{\tau_2}. \qquad (42)
\end{aligned}
$$

Let us call $\boldsymbol{v}_h^0 \equiv \boldsymbol{u}_h + \tau_1 \diamond \Pi_{\tau_1,0}(\boldsymbol{\xi}_h)$, $q_h^0 \equiv q_h + \tau_2 \diamond \Pi_{\tau_2,0}(\delta_h)$. Adding up (39) and (42), taking h small enough and α large enough ($\alpha > 3/2$) so that

$$
1 - \frac{3}{2\alpha}\big[1 + \psi(h)\big] - \frac{1}{2}\psi(h) \geqslant C_1 > 0,
$$

and using the stability condition (35), we obtain

$$
B_I\big([\boldsymbol{u}_h, p_h], \big[\boldsymbol{v}_h^0, q_h^0\big]\big) \geqslant C_1 \nu \|\nabla \boldsymbol{u}_h\|^2 + \left[\beta_0^2 C_1 - \frac{1}{2}\psi(h)\right]\big[\|\boldsymbol{\xi}_h\|^2_{\tau_1} + \|\delta_h\|^2_{\tau_2}\big],
$$

and therefore, if h is small enough,

$$
B_I\big([\boldsymbol{u}_h, p_h], \big[\boldsymbol{v}_h^0, q_h^0\big]\big) \geqslant C \big|\!\big|\!\big|[\boldsymbol{u}_h, p_h]\big|\!\big|\!\big|^2_I. \qquad (43)
$$

Please cite this article in press as: R. Codina, Analysis of a stabilized finite element approximation of the Oseen equations using orthogonal subscales, Applied Numerical Mathematics (2007), doi:10.1016/j.apnum.2006.11.011

On the other hand, using repeatedly the inverse estimate (26), the definition of τ_1 and τ_2, Lemma 2 and the fact that the norm of projection operators is $\leqslant 1$, it follows that

$$
\begin{aligned}
&\left|\!\left|\!\left|\left[\tau_1 \diamond \Pi_{\tau_1,0}(\boldsymbol{\xi}_h), \tau_2 \diamond \Pi_{\tau_2,0}(\delta_h)\right]\right|\!\right|\!\right|_I^2 \\
&\quad\leqslant \sum_K C\frac{C_{\mathrm{inv}}^2}{h_K^2}\left[1+\psi(h)\right]^2\left[\left(\nu\tau_{1,K}^2 + 2|\boldsymbol{a}|_{\infty,K}^2\tau_{1,K}^3 + \tau_{1,K}^2\tau_{2,K}\right)\left\|\Pi_{\tau_1,0}(\boldsymbol{\xi}_h)\right\|_K^2 + 2\tau_{1,K}\tau_{2,K}^2\left\|\Pi_{\tau_2,0}(\delta_h)\right\|_K^2\right] \\
&\quad\leqslant C\left(\|\boldsymbol{\xi}_h\|_{\tau_1}^2 + \|\delta_h\|_{\tau_2}^2\right) \\
&\quad\leqslant C\left|\!\left|\!\left|[\boldsymbol{u}_h, p_h]\right|\!\right|\!\right|_I^2,
\end{aligned}
$$

and therefore,

$$
\begin{aligned}
\left|\!\left|\!\left|\left[\boldsymbol{v}_h^0, q_h^0\right]\right|\!\right|\!\right|_I &\leqslant \left|\!\left|\!\left|[\boldsymbol{u}_h, p_h]\right|\!\right|\!\right|_I + \left|\!\left|\!\left|\left[\tau_1 \diamond \Pi_{\tau_1,0}(\boldsymbol{\xi}_h), \tau_2 \diamond \Pi_{\tau_2,0}(\delta_h)\right]\right|\!\right|\!\right|_I \\
&\leqslant C\left|\!\left|\!\left|[\boldsymbol{u}_h, p_h]\right|\!\right|\!\right|_I.
\end{aligned}
$$

The theorem follows using this in (43). □

Let $\boldsymbol{U}$ be the solution of the continuous problem. Since it verifies $B(\boldsymbol{U}, \boldsymbol{V}_h) = \langle \boldsymbol{f}, \boldsymbol{v}_h\rangle$ for all $\boldsymbol{V}_h \in \mathcal{W}_{h,0}$, it follows that

$$
B_I(\boldsymbol{U}, \boldsymbol{V}_h) = \langle \boldsymbol{f}, \boldsymbol{v}_h\rangle + \left(\Pi_{\tau_1}^{\perp}(\boldsymbol{a}\cdot\nabla\boldsymbol{u} + \nabla p), \boldsymbol{a}\cdot\nabla\boldsymbol{v}_h + \nabla q_h\right)_{\tau_1} + \left(\Pi_{\tau_2}^{\perp}(\nabla\cdot\boldsymbol{u}), \nabla\cdot\boldsymbol{v}_h\right)_{\tau_2}.
$$

Since $B_I(\boldsymbol{U}_h, \boldsymbol{V}_h) = \langle \boldsymbol{f}, \boldsymbol{v}_h\rangle$ it follows that

$$
B_I(\boldsymbol{U} - \boldsymbol{U}_h, \boldsymbol{V}_h) = \left(\Pi_{\tau_1}^{\perp}(\boldsymbol{a}\cdot\nabla\boldsymbol{u} + \nabla p), \boldsymbol{a}\cdot\nabla\boldsymbol{v}_h + \nabla q_h\right)_{\tau_1} + \left(\Pi_{\tau_2}^{\perp}(\nabla\cdot\boldsymbol{u}), \nabla\cdot\boldsymbol{v}_h\right)_{\tau_2}, \tag{44}
$$

from where we see that the method is *not consistent* in the classical variational sense, since the RHS of (44) is not zero. However, the consistency error can be bounded as follows:

Lemma 3 *(Bound for the consistency error of method I). Assume that hypothesis* H2, H5 *and* H6 *hold. Then, there is a constant C (in this case independent of $\boldsymbol{U}$) such that*

$$
B_I(\boldsymbol{U} - \boldsymbol{U}_h, \boldsymbol{V}_h) \leqslant C\varepsilon(h)|\!|\!|\boldsymbol{V}_h|\!|\!|_I \tag{45}
$$

for all $\boldsymbol{V}_h \in \mathcal{W}_{h,0}$.

Proof. From (44) we have that

$$
\begin{aligned}
&B_I(\boldsymbol{U} - \boldsymbol{U}_h, \boldsymbol{V}_h) \\
&\quad\leqslant C\|\boldsymbol{a}\cdot\nabla\boldsymbol{v}_h + \nabla q_h\|_{\tau_1}\left\|(\boldsymbol{a}\cdot\nabla\boldsymbol{u} + \nabla p) - \Pi_{\tau_1}(\boldsymbol{a}\cdot\nabla\boldsymbol{u} + \nabla p)\right\|_{\tau_1} + C\|\nabla\cdot\boldsymbol{v}_h\|_{\tau_2}\left\|(\nabla\cdot\boldsymbol{u}) - \Pi_{\tau_2}(\nabla\cdot\boldsymbol{u})\right\|_{\tau_2} \\
&\quad\leqslant C\left|\!\left|\!\left|[\boldsymbol{v}_h, q_h]\right|\!\right|\!\right|_I\left(\left\|\boldsymbol{a}\cdot\nabla\boldsymbol{u} - \Pi_{\tau_1}(\boldsymbol{a}\cdot\nabla\boldsymbol{u})\right\|_{\tau_1} + \left\|\nabla p - \Pi_{\tau_1}(\nabla p)\right\|_{\tau_1} + \left\|(\nabla\cdot\boldsymbol{u}) - \Pi_{\tau_2}(\nabla\cdot\boldsymbol{u})\right\|_{\tau_2}\right),
\end{aligned}
$$

for all $\boldsymbol{V}_h \in \mathcal{W}_{h,0}$. Let $v \in H^r(\Omega)$, $0 \leqslant r \leqslant k+1$, and let $\hat{v}_h$ be a finite element interpolant satisfying (30) for $m = 0$. Due to the best approximation property of the τ-projection Π_τ ($\tau = \tau_1$ or τ_2) with respect to the norm $\|\cdot\|_\tau$, we have that

$$
\left\|v - \Pi_\tau(v)\right\|_\tau \leqslant \|v - \hat{v}_h\|_\tau \leqslant C\sum_K \tau_K^{1/2}h_K^r\|v\|_{H^r(K)}, \tag{46}
$$

where we have used (31). The result follows now from this, the boundedness of the derivatives of $\boldsymbol{a}$ and the bounds (27)–(28) assumed for the constants c_i, which imply that $\tau_{1,K}$ behaves as $h_K^2\tau_{2,K}^{-1}$. □

Remark 3. There is a possible way to formulate the present method in a manner that it can be viewed as *consistent*. Indeed, if we introduce

$$
\begin{aligned}
&B_I^\star\left([\boldsymbol{u}_h, p_h, \boldsymbol{\xi}_h, \delta_h], [\boldsymbol{v}_h, q_h, \boldsymbol{\eta}_h, \gamma_h]\right) \\
&\quad := B\left([\boldsymbol{u}_h, p_h], [\boldsymbol{v}_h, q_h]\right) + (\boldsymbol{a}\cdot\nabla\boldsymbol{u}_h + \nabla p_h - \boldsymbol{\xi}_h, \boldsymbol{a}\cdot\nabla\boldsymbol{v}_h + \nabla q_h - \boldsymbol{\eta}_h)_{\tau_1} + (\nabla\cdot\boldsymbol{u}_h - \delta_h, \nabla\cdot\boldsymbol{v}_h - \gamma_h)_{\tau_2},
\end{aligned}
$$

Please cite this article in press as: R. Codina, Analysis of a stabilized finite element approximation of the Oseen equations using orthogonal subscales, Applied Numerical Mathematics (2007), doi:10.1016/j.apnum.2006.11.011

the discrete problem is equivalent to find $[\boldsymbol{u}_h, p_h, \boldsymbol{\xi}_h, \delta_h] \in \mathcal{V}_{h,0} \times \mathcal{Q}_{h,0} \times \mathcal{V}_h \times \mathcal{Q}_h$ such that $B_I^\star([\boldsymbol{u}_h, p_h, \boldsymbol{\xi}_h, \delta_h], [\boldsymbol{v}_h, q_h, \boldsymbol{\eta}_h, \gamma_h]) = \langle \boldsymbol{f}, \boldsymbol{v}_h \rangle$ for all $[\boldsymbol{v}_h, q_h, \boldsymbol{\eta}_h, \gamma_h] \in \mathcal{V}_{h,0} \times \mathcal{Q}_{h,0} \times \mathcal{V}_h \times \mathcal{Q}_h$. This problem is consistent in the sense that smooth enough solutions $[\boldsymbol{u}, p]$ of the continuous problem satisfy the discrete variational equation, $B_I^\star([\boldsymbol{u}, p, \boldsymbol{a} \cdot \nabla \boldsymbol{u} + \nabla p, \nabla \cdot \boldsymbol{u}], [\boldsymbol{v}_h, q_h, \boldsymbol{\eta}_h, \gamma_h]) = \langle \boldsymbol{f}, \boldsymbol{v}_h \rangle$.

Remark 4. Apart from the fact that the use of the weighted L^2 inner product defined by (13) and its associated projection arises naturally from the condition that the subscales be orthogonal to the finite element space, it turns out to be essential to establish the best approximation property used in (46).

The final result we need prior to proving convergence is:

Lemma 4 *(Estimates of the interpolation error of method I). Let $\boldsymbol{U} = [\boldsymbol{u}, p]$ be the solution of the continuous problem and $\hat{\boldsymbol{U}}_h = [\hat{\boldsymbol{u}}_h, \hat{p}_h]$ a finite element interpolant of $\boldsymbol{U}$ satisfying* (30)*, and assume that* H1, H5 *and* H6 *hold. Then*

$$B_I(\boldsymbol{U} - \hat{\boldsymbol{U}}_h, \boldsymbol{V}_h) \leqslant C\varepsilon(h) |||\boldsymbol{V}_h|||_I, \quad \forall \boldsymbol{V}_h \in \mathcal{W}_{h,0}, \tag{47}$$

$$|||\boldsymbol{U} - \hat{\boldsymbol{U}}_h|||_I \leqslant C\varepsilon(h). \tag{48}$$

Proof. Let $\hat{\boldsymbol{e}}_u := \boldsymbol{u} - \hat{\boldsymbol{u}}_h$ and $\hat{e}_p := p - \hat{p}_h$ be the finite element interpolation errors for the velocity and the pressure, respectively. From the definition (20) of B_I we have that

$$\begin{aligned} B_I(\boldsymbol{U} - \hat{\boldsymbol{U}}_h, \boldsymbol{V}_h) = {} & \nu(\nabla \hat{\boldsymbol{e}}_u, \nabla \boldsymbol{v}_h) + (\boldsymbol{a} \cdot \nabla \hat{\boldsymbol{e}}_u, \boldsymbol{v}_h) - (\hat{e}_p, \nabla \cdot \boldsymbol{v}_h) + (q_h, \nabla \cdot \hat{\boldsymbol{e}}_u) \\ & + \big(\Pi_{\tau_1}^\perp(\boldsymbol{a} \cdot \nabla \hat{\boldsymbol{e}}_u + \nabla \hat{e}_p), \boldsymbol{a} \cdot \nabla \boldsymbol{v}_h + \nabla q_h\big)_{\tau_1} + \big(\Pi_{\tau_2}^\perp(\nabla \cdot \hat{\boldsymbol{e}}_u), \nabla \cdot \boldsymbol{v}_h\big)_{\tau_2}. \end{aligned}$$

Let us check that each of these terms satisfies estimate (47). For the first we have

$$\begin{aligned} \nu(\nabla \hat{\boldsymbol{e}}_u, \nabla \boldsymbol{v}_h) &\leqslant C\nu^{1/2} \|\nabla \boldsymbol{v}_h\| \sum_K \frac{\nu^{1/2}}{h_K} h_K^{k+1} \|\boldsymbol{u}\|_{k+1,K} \\ &\leqslant C |||\boldsymbol{V}_h|||_I \sum_K \tau_{1,K}^{-1/2} h_K^{k+1} \|\boldsymbol{u}\|_{k+1,K}. \end{aligned}$$

Adding up the second and the fourth terms and integrating by parts we get

$$\begin{aligned} (\boldsymbol{a} \cdot \nabla \hat{\boldsymbol{e}}_u, \boldsymbol{v}_h) + (q_h, \nabla \cdot \hat{\boldsymbol{e}}_u) &= -(\hat{\boldsymbol{e}}_u, \boldsymbol{a} \cdot \nabla \boldsymbol{v}_h + \nabla q_h) \\ &\leqslant C \sum_K \tau_{1,K}^{1/2} \|\boldsymbol{a} \cdot \nabla \boldsymbol{v}_h + \nabla q_h\|_K \tau_{1,K}^{-1/2} \|\hat{\boldsymbol{e}}_u\|_K \\ &\leqslant C |||\boldsymbol{V}_h|||_I \sum_K \tau_{1,K}^{-1/2} h_K^{k+1} \|\boldsymbol{u}\|_{k+1,K}. \end{aligned}$$

Note that H6 implies that $\boldsymbol{u}$ is continuous ($d = 2, 3$) and $\hat{\boldsymbol{u}}_h$ can be taken as the standard nodal interpolant. Thus, $\hat{\boldsymbol{e}}_u$ vanishes on $\partial\Omega$. The third term can be bounded as

$$\begin{aligned} -(\hat{e}_p, \nabla \cdot \boldsymbol{v}_h) &\leqslant C \sum_K \tau_{2,K}^{1/2} \|\nabla \cdot \boldsymbol{v}_h\|_K \tau_{2,K}^{-1/2} \|\hat{e}_p\|_K \\ &\leqslant C |||\boldsymbol{V}_h|||_I \sum_K \tau_{2,K}^{-1/2} h_K^k \|p\|_{k,K}. \end{aligned}$$

Using the fact that the norm of projection operators is $\leqslant 1$ we obtain the following bound for the fifth term

$$\begin{aligned} \big(\Pi_{\tau_1}^\perp(\boldsymbol{a} \cdot \nabla \hat{\boldsymbol{e}}_u + \nabla \hat{e}_p), \boldsymbol{a} \cdot \nabla \boldsymbol{v}_h + \nabla q_h\big)_{\tau_1} &\leqslant C |||\boldsymbol{V}_h|||_I \sum_K \tau_{1,K}^{1/2} \left(\frac{|\boldsymbol{a}|_{\infty,K}}{h_K} h_K^{k+1} \|\boldsymbol{u}\|_{k+1,K} + \frac{1}{h_K} h_K^k \|p\|_{k,K} \right) \\ &\leqslant C |||\boldsymbol{V}_h|||_I \sum_K \big(\tau_{1,K}^{-1/2} h_K^{k+1} \|\boldsymbol{u}\|_{k+1,K} + \tau_{2,K}^{-1/2} h_K^k \|p\|_{k,K} \big). \end{aligned}$$

Likewise

Please cite this article in press as: R. Codina, Analysis of a stabilized finite element approximation of the Oseen equations using orthogonal subscales, Applied Numerical Mathematics (2007), doi:10.1016/j.apnum.2006.11.011

$$\big(\Pi_{\tau_2}^{\perp}(\nabla\cdot\hat{\boldsymbol{e}}_u),\nabla\cdot\boldsymbol{v}_h\big)_{\tau_2}\leqslant C\|\nabla\cdot\boldsymbol{v}_h\|_{\tau_2}\sum_K\frac{\tau_{2,K}^{1/2}}{h_K}h_K^{k+1}\|\boldsymbol{u}\|_{k+1,K}$$
$$\leqslant C|||\boldsymbol{V}_h|||_I\sum_K\tau_{1,K}^{-1/2}h_K^{k+1}\|\boldsymbol{u}\|_{k+1,K},$$

which completes the proof of (47). Estimate (48) can be proved in a similar manner. □

Now we are ready to prove the convergence result:

Theorem 2 *(Convergence of method I). Under assumptions* H1–H6*, for h small enough there is a constant C (independent of* $\boldsymbol{U}$*) such that*

$$|||\boldsymbol{U}-\boldsymbol{U}_h|||_I\leqslant C\varepsilon(h).$$

Proof. The proof is standard: from Theorem 1 and using Lemmas 3 and 4 (estimate (47)), there exists $\boldsymbol{V}_h\in\mathcal{W}_{h,0}$ such that

$$\beta_I|||\hat{\boldsymbol{U}}_h-\boldsymbol{U}_h|||_I|||\boldsymbol{V}_h|||_I\leqslant B_I(\hat{\boldsymbol{U}}_h-\boldsymbol{U},\boldsymbol{V}_h)+B_I(\boldsymbol{U}-\boldsymbol{U}_h,\boldsymbol{V}_h)$$
$$\leqslant C\varepsilon(h)|||\boldsymbol{V}_h|||_I,$$

and therefore $|||\hat{\boldsymbol{U}}_h-\boldsymbol{U}_h|||_I\leqslant C\varepsilon(h)$. The result follows now from Lemma 4 (estimate (48)) and the triangle inequality. □

3.3. Method II

Now the problem is: find $\boldsymbol{U}_h\in\mathcal{W}_{h,0}$ such that $B_{II}(\boldsymbol{U}_h,\boldsymbol{V}_h)=\langle\boldsymbol{f},\boldsymbol{v}_h\rangle$ for all $\boldsymbol{V}_h\in\mathcal{W}_{h,0}$, with B_{II} defined in (21). The norm in which we will prove stability and convergence is now

$$|||\boldsymbol{V}_h|||_{II}\equiv\big|||[\boldsymbol{v}_h,q_h]\big|||_{II}:=\big|||[\boldsymbol{v}_h,q_h]\big|||_I+\big\|\Pi_{\tau_1}^{\perp}(\boldsymbol{a}\cdot\nabla\boldsymbol{v}_h)\big\|_{\tau_1}+\big\|\Pi_{\tau_1}^{\perp}(\nabla q_h)\big\|\tau_1.\tag{49}$$

It is observed that this norm is slightly finer than $|||\cdot|||_I$. Now we will have control over the orthogonal component of both the convective derivative of the velocity and the pressure gradient. However, we still do not have control over all the components of these two vectors separately (see the following subsection).

Theorem 3 *(Stability of method II). Under the same assumptions as in Theorem* 1*, there is a constant* $\beta_{II}>0$ *such that*

$$\inf_{\boldsymbol{U}_h\in\mathcal{W}_{h,0}}\sup_{\boldsymbol{V}_h\in\mathcal{W}_{h,0}}\frac{B_{II}(\boldsymbol{U}_h,\boldsymbol{V}_h)}{|||\boldsymbol{U}_h|||_{II}|||\boldsymbol{V}_h|||_{II}}\geqslant\beta_{II}.$$

Proof. Let us proceed exactly as in the proof of Theorem 1. Using the inequality $a^2+b^2\geqslant(a^2+b^2)/3+(a+b)^2/3$, it is found that instead of (39) we now have

$$B_{II}\big([\boldsymbol{u}_h,p_h],[\boldsymbol{u}_h,p_h]\big)\geqslant\nu\|\nabla\boldsymbol{u}_h\|^2+\frac{1}{3}\big\|\Pi_{\tau_1}^{\perp}(\boldsymbol{\xi}_h)\big\|_{\tau_1}^2+\big\|\Pi_{\tau_2}^{\perp}(\delta_h)\big\|_{\tau_2}^2+\frac{1}{3}\big\|\Pi_{\tau_1}^{\perp}(\boldsymbol{a}\cdot\nabla\boldsymbol{u}_h)\big\|_{\tau_1}^2+\frac{1}{3}\big\|\Pi_{\tau_1}^{\perp}(\nabla p_h)\big\|_{\tau_1}^2.$$

Once again, the bilinear form B_{II} is not coercive in the norm (49). If now we take $[\boldsymbol{v}_h,q_h]=[\tau_1\diamond\Pi_{\tau_1,0}(\boldsymbol{\xi}_h),\tau_2\diamond\Pi_{\tau_2,0}(\delta_h)]$, an expression similar to (40) is found. Only the sixth and seventh terms of the RHS of this inequality are different. They and their bounds in (41) have to be replaced by

$$\big(\boldsymbol{a}\cdot\nabla\big[\tau_1\diamond\Pi_{\tau_1,0}(\boldsymbol{\xi}_h)\big],\Pi_{\tau_1}^{\perp}(\boldsymbol{a}\cdot\nabla\boldsymbol{u}_h)\big)_{\tau_1}+\big(\nabla\big[\tau_2\diamond\Pi_{\tau_2,0}(\delta_h)\big],\Pi_{\tau_1}^{\perp}(\nabla p_h)\big)_{\tau_1}$$
$$\geqslant-\sum_K\frac{C_{\mathrm{inv}}}{h_K}|\,\boldsymbol{a}\,|_{\infty,K}\,\tau_{1,K}\big\|\tau_1\diamond\Pi_{\tau_1,0}(\boldsymbol{\xi}_h)\big\|_K\big\|\Pi_{\tau_1}^{\perp}(\boldsymbol{a}\cdot\nabla\boldsymbol{u}_h)\big\|_K$$
$$-\sum_K\frac{C_{\mathrm{inv}}}{h_K}\tau_{1,K}\big\|\tau_2\diamond\Pi_{\tau_2,0}(\delta_h)\big\|_K\big\|\Pi_{\tau_1}^{\perp}(\nabla p_h)\big\|_K.$$

Please cite this article in press as: R. Codina, Analysis of a stabilized finite element approximation of the Oseen equations using orthogonal subscales, Applied Numerical Mathematics (2007), doi:10.1016/j.apnum.2006.11.011

Calling again $\boldsymbol{v}_h^0 \equiv \boldsymbol{u}_h + \tau_1 \diamond \Pi_{\tau_1,0}(\boldsymbol{\xi}_h)$, $q_h^0 \equiv q_h + \tau_2 \diamond \Pi_{\tau_2,0}(\delta_h)$, it is found now that

$$
\begin{aligned}
&B_I\big([\boldsymbol{u}_h, p_h], [\boldsymbol{v}_h^0, q_h^0]\big) \\
&\geqslant \left[1 - \frac{1}{2\alpha}\big[1+\psi(h)\big]\right]\nu\|\nabla \boldsymbol{u}_h\|^2 + \left[1 - \frac{3}{2\alpha}\big[1+\psi(h)\big] - \frac{1}{2}\psi(h)\right]\big\|\Pi_{\tau_1,0}(\boldsymbol{\xi}_h)\big\|_{\tau_1}^2 \\
&\quad + \frac{1}{3}\big\|\Pi_{\tau_1}^{\perp}(\boldsymbol{\xi}_h)\big\|_{\tau_1}^2 - \frac{1}{2}\psi(h)\|\boldsymbol{\xi}_h\|_{\tau_1}^2 + \left[\frac{1}{3} - \frac{1}{2\alpha}\big[1+\psi(h)\big]\right]\big\|\Pi_{\tau_1}^{\perp}(\boldsymbol{a}\cdot\nabla \boldsymbol{u}_h)\big\|_{\tau_1}^2 \\
&\quad + \left[\frac{1}{3} - \frac{1}{2\alpha}\big[1+\psi(h)\big]\right]\big\|\Pi_{\tau_1}^{\perp}(\nabla p_h)\big\|_{\tau_1}^2 + \left[1 - \frac{1}{2\alpha}\big[1+\psi(h)\big] - \frac{1}{2}\psi(h)\right]\big\|\Pi_{\tau_2,0}(\delta_h)\big\|_{\tau_2}^2 \\
&\quad + \left[1 - \frac{1}{2\alpha}\big[1+\psi(h)\big]\right]\big\|\Pi_{\tau_2}^{\perp}(\delta_h)\big\|_{\tau_1}^2 - \frac{1}{2}\psi(h)\|\delta_h\|_{\tau_2}^2.
\end{aligned}
$$

From this and (35) it follows that for h small enough there is an $\alpha > 1$ for which

$$B_{II}\big([\boldsymbol{u}_h, p_h], [\boldsymbol{v}_h^0, q_h^0]\big) \geqslant C\,|||[\boldsymbol{u}_h, p_h]|||_{II}^2.$$

Similar bounds to those employed in Theorem 1 yield

$$
\begin{aligned}
|||\big[\tau_1 \diamond \Pi_{\tau_1,0}(\boldsymbol{\xi}_h), \tau_2 \diamond \Pi_{\tau_2,0}(\delta_h)\big]|||_{II}^2 &\leqslant C\big(\|\boldsymbol{\xi}_h\|_{\tau_1}^2 + \|\delta_h\|_{\tau_2}^2\big) \\
&\leqslant C\,|||[\boldsymbol{u}_h, p_h]|||_{II}^2,
\end{aligned}
$$

and the proof concludes as in Theorem 1. □

The consistency error of method II is

$$B_{II}(\boldsymbol{U} - \boldsymbol{U}_h, \boldsymbol{V}_h) = \big(\Pi_{\tau_1}^{\perp}(\boldsymbol{a}\cdot\nabla \boldsymbol{u}), \boldsymbol{a}\cdot\nabla \boldsymbol{v}_h\big)_{\tau_1} + \big(\Pi_{\tau_1}^{\perp}(\nabla p), \nabla q_h\big)_{\tau_1} + \big(\Pi_{\tau_2}^{\perp}(\nabla\cdot\boldsymbol{u}), \nabla\cdot\boldsymbol{v}_h\big)_{\tau_2}.$$

The bound (45) of Lemma 3 also holds for this case, as well as the estimates for the interpolation error given in (47) and (48). The proof of all these facts follows the same lines as for method I, only with minor modifications. We give directly the convergence result, whose proof is also straightforward:

Theorem 4 *(Convergence of method II). Under the same assumptions as in Theorem* 2*, there is a constant* C *(independent of* $\boldsymbol{U}$*) such that*

$$|||\boldsymbol{U} - \boldsymbol{U}_h|||_{II} \leqslant C\varepsilon(h),$$

where $\varepsilon(h)$ *is the same error function as for method I, given by* (36)*.*

3.4. Viscous dominated case

Both in methods I and II the stability result obtained shows that $\boldsymbol{a}\cdot\nabla \boldsymbol{u}_h + \nabla p_h$ is under control. However, we do not have explicit bounds over these two terms (and their errors) separately. Nevertheless, there is the possibility of bounding the pressure gradient making use of the control over the viscous term, since

$$
\begin{aligned}
\tau_{1,K}\|\nabla p_h\|_K^2 &\leqslant \tau_{1,K}\|\boldsymbol{a}\cdot\nabla \boldsymbol{u}_h + \nabla p_h\|_K^2 + \tau_{1,K}\|\boldsymbol{a}\cdot\nabla \boldsymbol{u}_h\|_K^2 \\
&\leqslant \tau_{1,K}\|\boldsymbol{a}\cdot\nabla \boldsymbol{u}_h + \nabla p_h\|_K^2 + C\left(\frac{|\boldsymbol{a}|_{\infty,K}h_K}{\nu}\right)\nu\|\nabla \boldsymbol{u}_h\|_K^2. \qquad (50)
\end{aligned}
$$

Let us introduce the dimensionless quantities

$$Re := \frac{|\boldsymbol{a}|_\infty L}{\nu}, \qquad Re_K := \frac{|\boldsymbol{a}|_{\infty,K}h_K}{\nu}, \qquad Re_h := \max\{Re_K \mid K \in \mathcal{P}_h\},$$

where L is a characteristic length of Ω. These numbers may be called the *global*, *cell* and *mesh Reynolds numbers*, respectively.

From (50) it is seen that we have control over $\tau_{1,K}\|\nabla p_h\|_K^2$, but with a constant depending on the inverse of Re_K. Therefore, this estimate is numerically meaningful only for small values of Re_K. However, if we allow our stability

Please cite this article in press as: R. Codina, Analysis of a stabilized finite element approximation of the Oseen equations using orthogonal subscales, Applied Numerical Mathematics (2007), doi:10.1016/j.apnum.2006.11.011

and error estimates to depend on this parameter, it is not necessary to use neither method I nor method II, but rather a simplified form of these which does not include the stabilizing term for the velocity streamline derivative. This method consists of finding $\boldsymbol{U}_h \in \mathcal{W}_{h,0}$ such that $B_\nu(\boldsymbol{U}_h, \boldsymbol{V}_h) = \langle \boldsymbol{f}, \boldsymbol{v}_h \rangle$ for all $\boldsymbol{V}_h \in \mathcal{W}_{h,0}$, with B_ν defined as

$$B_\nu(\boldsymbol{U}_h, \boldsymbol{V}_h) = B(\boldsymbol{U}_h, \boldsymbol{V}_h) + \big(\Pi_\tau^\perp(\nabla p_h), \nabla q_h\big)_\tau, \tag{51}$$

and with B given in (4). Clearly, the only purpose of this method is to stabilize the pressure. The behavior in convective dominated situations will be similar to that of the standard Galerkin method using div-stable velocity–pressure interpolations.

Except for the presence of the convective term in B, this formulation is the same as that introduced in [18]. We will present here a different stability proof which furthermore will show the dependence of the stability and error estimates on Re_h and Re. For that, let us introduce the norm

$$|||\boldsymbol{V}_h|||_\nu \equiv \big|||[\boldsymbol{v}_h, q_h]|||_\nu := \nu^{1/2}\|\nabla \boldsymbol{v}_h\| + \frac{1}{1+Re_h}\|\nabla q_h\|_\tau + \frac{1}{1+Re}\frac{1}{\nu^{1/2}}\|q_h\|, \tag{52}$$

in which the analysis of the method will be performed. Now the parameters τ_K, which correspond to $\tau_{1,K}$ of the previous methods, can be taken as

$$\tau_K = \frac{h_{K,\min}^2}{\alpha^2 C_{\text{inv}}^2 \nu}, \tag{53}$$

and $\tau_{2,K}$ simply set to zero.

Theorem 5 *(Stability of the viscous dominated case). Assume that* H3 *and* H4 *hold, and the parameters τ_K are given by* (53)*. Then, for h sufficiently small there is a constant $\beta_\nu > 0$ such that*

$$\inf_{\boldsymbol{U}_h \in \mathcal{W}_{h,0}} \sup_{\boldsymbol{V}_h \in \mathcal{W}_{h,0}} \frac{B_\nu(\boldsymbol{U}_h, \boldsymbol{V}_h)}{|||\boldsymbol{U}_h|||_\nu |||\boldsymbol{V}_h|||_\nu} \geqslant \beta_\nu. \tag{54}$$

Proof. The proof of this result is similar to the proofs of Theorems 1 and 3, except for the presence of the L^2 norm of q_h in the definition (52). Now we have that

$$B_\nu\big([\boldsymbol{u}_h, p_h], [\boldsymbol{u}_h, p_h]\big) = \nu\|\nabla \boldsymbol{u}_h\|^2 + \big\|\Pi_\tau^\perp(\nabla p_h)\big\|_\tau^2, \tag{55}$$

and, using the same strategy as in Theorem 1,

$$\begin{aligned}
&B_\nu\big([\boldsymbol{u}_h, p_h], \big[\tau \diamond \Pi_{\tau,0}(\nabla p_h), 0\big]\big) \\
&\quad = \nu\big(\nabla \boldsymbol{u}_h, \nabla\big[\tau \diamond \Pi_{\tau,0}(\nabla p_h)\big]\big) + \big(\boldsymbol{a}\cdot\nabla \boldsymbol{u}_h, \tau \diamond \Pi_{\tau,0}(\nabla p_h)\big) \\
&\qquad + \big(\nabla p_h, \tau \circ \Pi_{\tau,0}(\nabla p_h)\big) + \big(\nabla p_h, \tau \diamond \Pi_{\tau,0}(\nabla p_h) - \tau \circ \Pi_{\tau,0}(\nabla p_h)\big) \\
&\quad \geqslant -\sum_K \nu \frac{C_{\text{inv}}}{h_K}\|\nabla \boldsymbol{u}_h\|_K \big\|\tau \diamond \Pi_{\tau,0}(\nabla p_h)\big\|_K - \sum_K |\boldsymbol{a}|_{\infty,K}\|\nabla \boldsymbol{u}_h\|_K \big\|\tau \diamond \Pi_{\tau,0}(\nabla p_h)\big\|_K \\
&\qquad + \big\|\Pi_{\tau,0}(\nabla p_h)\big\|_\tau^2 - \sum_K \|\nabla p_h\|_K \big\|\tau \diamond \Pi_{\tau,0}(\nabla p_h) - \tau \circ \Pi_{\tau,0}(\nabla p_h)\big\|_K.
\end{aligned}$$

Noting that $\tau_K |\boldsymbol{a}|_{\infty,K}^2 \leqslant C\nu Re_h^2$ and using Lemma 2, it is not difficult to see that this last inequality can be written as

$$B_\nu\big([\boldsymbol{u}_h, p_h], \big[\tau \diamond \Pi_{\tau,0}(\nabla p_h), 0\big]\big) \geqslant C_1\big\|\Pi_{\tau,0}(\nabla p_h)\big\|_\tau^2 - C_2\psi(h)\|\nabla p_h\|_\tau^2 - C_3\big(1+Re_h^2\big)\nu\|\nabla \boldsymbol{u}_h\|^2, \tag{56}$$

where the constants C_i, $i = 1, 2, 3$, do not depend neither on Re_h nor on Re. To introduce the L^2 norm of p_h, let us invoke the inf–sup condition for the continuous problem, namely, the continuous counterpart of condition (7). Since p_h belongs to $L^2(\Omega)$, there exists a function $\boldsymbol{v} \in \mathcal{V}_0$ such that

$$\beta\|p_h\|\|\nabla \boldsymbol{v}\| \leqslant \big|(p_h, \nabla\cdot\boldsymbol{v})\big|.$$

We have used the L^2 norm of $\nabla \boldsymbol{v}$ in the LHS since due to the Poincaré–Friedrics inequality it is equivalent to the H^1 norm of $\boldsymbol{v}$. We may thus normalize $\boldsymbol{v}$ so that $\|\nabla \boldsymbol{v}\| = \|p_h\|/\nu$. Let now $\hat{\boldsymbol{v}}_h$ be a finite element interpolant of $\boldsymbol{v}$ satisfying (30). Using the fact that $|a-b| \geqslant |a| - |b|$, we have:

$$B_\nu\big([\boldsymbol{u}_h, p_h], [\hat{\boldsymbol{v}}_h, 0]\big) = \big|\nu(\nabla \boldsymbol{u}_h, \nabla \hat{\boldsymbol{v}}_h) + (\boldsymbol{a}\cdot\nabla \boldsymbol{u}_h, \hat{\boldsymbol{v}}_h) - (p_h, \nabla\cdot\hat{\boldsymbol{v}}_h)\big|$$
$$\geqslant \big|(p_h, \nabla\cdot\boldsymbol{v})\big| - \big|\big(p_h, \nabla\cdot(\boldsymbol{v}-\hat{\boldsymbol{v}}_h)\big)\big| - \big|\nu(\nabla \boldsymbol{u}_h, \nabla \hat{\boldsymbol{v}}_h)\big| - \big|(\boldsymbol{a}\cdot\nabla \boldsymbol{u}_h, \hat{\boldsymbol{v}}_h)\big|. \tag{57}$$

If C_L denotes the constant of the Poincaré–Friedrics inequality and C_I the constant in the interpolation estimates (30), we have that

$$\|\boldsymbol{v}-\hat{\boldsymbol{v}}_h\|_K \leqslant C_I \sum_{K'\subset S_K} h_{K'}\|\nabla \boldsymbol{v}\|_{K'},$$
$$\|\nabla\hat{\boldsymbol{v}}_h\| \leqslant \|\nabla\boldsymbol{v}-\nabla\hat{\boldsymbol{v}}_h\| + \|\nabla\boldsymbol{v}\| \leqslant C\|\nabla\boldsymbol{v}\| = C\frac{1}{\nu}\|p_h\|,$$
$$\|\hat{\boldsymbol{v}}_h\| \leqslant C_L\|\nabla\hat{\boldsymbol{v}}_h\| \leqslant C_L C\frac{1}{\nu}\|p_h\|.$$

Integrating by parts the second term in (57), using these bounds and the quasi-uniformity of the patches S_K, we obtain

$$B_\nu\big([\boldsymbol{u}_h, p_h], [\hat{\boldsymbol{v}}_h, 0]\big)$$
$$\geqslant \beta\frac{1}{\nu}\|p_h\|^2 - \sum_K \|\nabla p_h\|_K\|\boldsymbol{v}-\hat{\boldsymbol{v}}_h\|_K - \nu\|\nabla\boldsymbol{u}_h\|\|\nabla\hat{\boldsymbol{v}}_h\| - |\boldsymbol{a}|_\infty\|\nabla\boldsymbol{u}_h\|\hat{\boldsymbol{v}}_h\|$$
$$\geqslant \beta\frac{1}{\nu}\|p_h\|^2 - C\sum_K h_K\|\nabla p_h\|_K\|\nabla\boldsymbol{v}\|_K - C\|\nabla\boldsymbol{u}_h\|\|p_h\| - |\boldsymbol{a}|_\infty C_L C\frac{1}{\nu}\|\nabla\boldsymbol{u}_h\|\|p_h\|. \tag{58}$$

On the other hand, from Young's inequality we have that

$$\sum_K h_K\|\nabla p_h\|_K\|\nabla\boldsymbol{v}\|_K \leqslant \sum_K\left[\frac{h_K^2}{2\nu\epsilon}\|\nabla p_h\|_K^2 + \frac{\nu\epsilon}{2}\|\nabla\boldsymbol{v}\|_K^2\right]$$
$$\leqslant \frac{C}{\epsilon}\|\nabla p_h\|_\tau^2 + \frac{\epsilon}{2\nu}\|p_h\|^2,$$

for all $\epsilon > 0$. Using a similar inequality for the last two terms of (58), taking ϵ small enough and noting that since C_L is proportional to L, $|\boldsymbol{a}|_\infty C_L/\nu$ is proportional to Re, we obtain

$$B_\nu\big([\boldsymbol{u}_h, p_h], [\hat{\boldsymbol{v}}_h, 0]\big) \geqslant C_4\frac{1}{\nu}\|p_h\|^2 - C_5\|\nabla p_h\|_\tau^2 - C_6\big(1+Re^2\big)\nu\|\nabla\boldsymbol{u}_h\|^2, \tag{59}$$

for constants C_4, C_5 and C_6 independent of Re_h and Re. If now we take

$$\boldsymbol{v}_h^0 \equiv \boldsymbol{u}_h + \frac{A_1}{1+Re_h^2}\tau\diamond\Pi_{\tau,0}(\nabla p_h) + \frac{A_2}{1+Re^2}\hat{\boldsymbol{v}}_h,$$
$$q_h^0 \equiv p_h, \tag{60}$$

and add up (55), (56) and (59) multiplied by the corresponding coefficients, we obtain

$$B_\nu\big([\boldsymbol{u}_h, p_h], \big[\boldsymbol{v}_h^0, q_h^0\big]\big) \geqslant [1 - C_3A_1 - C_6A_2]\nu\|\nabla\boldsymbol{u}_h\|^2 + \left[1 - \frac{C_2\psi(h)}{1+Re_h^2}\frac{A_1}{\beta_0} - \frac{C_5}{1+Re^2}\frac{A_2}{\beta_0}\right]\big\|\Pi_\tau^\perp(\nabla p_h)\big\|_\tau^2$$
$$+ \left[\frac{C_1A_1}{1+Re_h^2} - \frac{C_2\psi(h)}{1+Re_h^2}\frac{A_1}{\beta_0} - \frac{C_5}{1+Re^2}\frac{A_2}{\beta_0}\right]\big\|\Pi_{\tau,0}(\nabla p_h)\big\|_\tau^2 + \left[\frac{C_4}{\nu}\frac{A_2}{1+Re^2}\right]\|p_h\|^2$$

where we have made use of the stability condition (35) (now with $\boldsymbol{z}_h = \nabla p_h$). From this, it follows that there are values of the constants A_1 and A_2 for which

$$B_\nu\big([\boldsymbol{u}_h, p_h], \big[\boldsymbol{v}_h^0, q_h^0\big]\big) \geqslant C\big|\!\big|\!\big|[\boldsymbol{u}_h, p_h]\big|\!\big|\!\big|_\nu^2.$$

The theorem now follows after checking that

$$\big|\!\big|\!\big|\big[\boldsymbol{v}_h^0, q_h^0\big]\big|\!\big|\!\big|_\nu \leqslant C\big|\!\big|\!\big|[\boldsymbol{u}_h, p_h]\big|\!\big|\!\big|_\nu,$$

which is easily verified from the definition (60) of $[\boldsymbol{v}_h^0, q_h^0]$ and noting that $(1+x^2)^{-1} \leqslant 2(1+x)^{-1}$ for all $x > 0$. □

Please cite this article in press as: R. Codina, Analysis of a stabilized finite element approximation of the Oseen equations using orthogonal subscales, Applied Numerical Mathematics (2007), doi:10.1016/j.apnum.2006.11.011

The same strategy as for methods I and II can now be followed to prove convergence. We omit the intermediate steps and simply state the final result:

Theorem 6 *(Convergence of the viscous dominated case). If assumptions* H1–H5 *hold and the parameters* τ_K *are given by* (53)*, for h small enough there is a constant C* (*independent of* $\boldsymbol{U}$) *such that*

$$|||\boldsymbol{U}-\boldsymbol{U}_h|||_\nu \leqslant C(1+Re_h)\sum_K \big(\tau_K^{-1/2}h_K^{k+1}\|\boldsymbol{u}\|_{k+1,K}+\nu^{-1/2}h_K^k\|p\|_{k,K}\big).$$

This convergence estimate, as well as the stability estimate (54), deteriorates as ν decreases. Due to the dependence on Re_h and *Re explicitly displayed* by (52), it is seen that control over the L^2 norm of the pressure is rapidly lost as $\nu \to 0$, since in this case $Re \to \infty$. However, a somewhat stronger control is obtained on $\|\nabla q_h\|_\tau$. We may consider that the finite element mesh is sufficiently refined so as to maintain Re_h (relatively) small. These results are similar to those obtained in [30] for the nonlinear Navier–Stokes equations, even though the method analyzed in this reference is also intended to stabilize convection.

Remark 5. In the absence of convection, the norm (52) in which stability and convergence has been proven is even finer than for the Galerkin method using div-stable velocity–pressure interpolations. This in particular allows to extend this pressure stabilized method to the nonlinear Navier–Stokes equations and obtain *exactly* the same results as for the Galerkin method (see [11,24]). This extension is analyzed in [19] for the stationary problem and in [3] for the transient case.

Remark 6. In [8] a method similar to the one presented here *for the Stokes problem* is put as example of a general stabilization procedure. It is claimed there that optimal error estimates are obtained if τ_K is taken of order $\mathcal{O}(1)$ instead of given by (53). However, this is possible only if pressures are at least of the *same* regularity as the velocities.

4. Numerical results

In this section we compare the numerical results obtained with the first stabilized formulation analyzed in this paper, given by (19), and the algebraic subgrid scale method, given by (14), in two simple bidimensional examples. We will use the acronym OSS for the former (standing for orthogonal subscale stabilization) and ASGS for the latter. The stabilization parameters used are the same in both formulations, with the constants in (11)–(12) taken as $c_1 = 4$, $c_2 = 2$, $c_3 = 1$, $c_4 = 1/2$, and $h_{K,\min}$ as the length of the element side for bilinear elements and half of it for biquadratic elements, the two interpolation types considered.

4.1. Flow in an L-shaped domain

The purpose of this example is to check the performance of the OSS method in a simple example but showing three features of practical interest: the presence of internal layers, of boundary layers and high pressure variations.

The computational domain is taken as the interior of $[0,3]\times[0,3]\setminus[0,2]\times[1,3]$. The inlet is taken at $x=0$, where a discontinuous inflow velocity $\boldsymbol{u}=(1,0)$ for $0\leqslant y\leqslant 1/2$ and $\boldsymbol{u}=(0,0)$ for $1/2<y\leqslant 1$ is prescribed. A zero pressure is prescribed at the outlet $y=3$ and on the rest of the boundary $\boldsymbol{u}$ is fixed to $(0,0)$. The Oseen equations (1)–(2) are solved, taking $\boldsymbol{a}=(1,0)$ and $\nu=10^{-4}$. For such a small viscosity, the inflow discontinuous profile propagates inwards with little smearing and a velocity boundary layer is created at $x=3$. It has to be noted that since the boundary data are discontinuous the velocity components do not belong to $H^1(\Omega)$. Nevertheless, this test is intended not to check convergence, but as an example of a problem with internal layers.

The domain is discretized using 2000 biquadratic elements of equal size, yielding 8241 nodal points. For these elements, second-order derivatives cannot be neglected in the ASGS method (14).

Pressure contours and velocity vectors are shown in Fig. 1. These results have been obtained using the ASGS method, and are very similar to those obtained using the OSS formulation. The differences are observed in Fig. 2. Three main conclusions can be drawn from these. First, internal layers are approximated similarly, with the same overshoots and undershoots in both methods. This could be expected, since both the ASGS and OSS introduce streamline diffusion, but no crosswind numerical dissipation. From the y-velocity section at $y=2$ it is seen that the OSS

Please cite this article in press as: R. Codina, Analysis of a stabilized finite element approximation of the Oseen equations using orthogonal subscales, Applied Numerical Mathematics (2007), doi:10.1016/j.apnum.2006.11.011

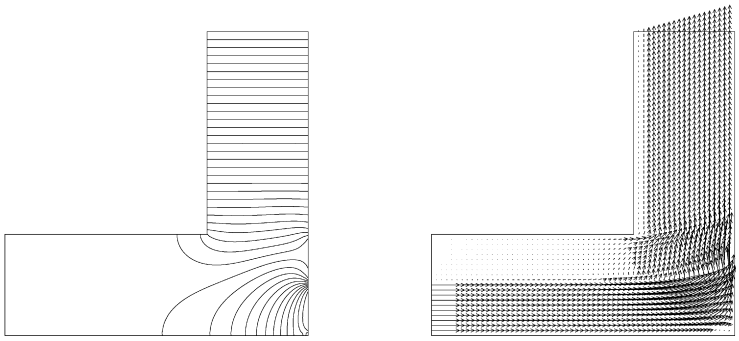

Fig. 1. Pressure contours (left) and velocity vectors (right) for the flow in an L-shaped domain.

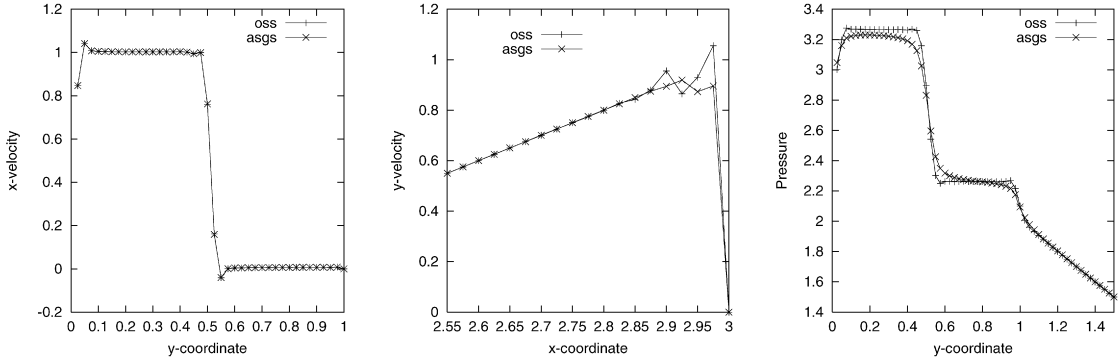

Fig. 2. x-velocity at $x = 1$ (left), y-velocity at $y = 2$ (middle) and pressure at $x = 3$ (right) for the flow in an L-shaped domain.

yields more oscillations near the boundary layer, which are due to the fact that it introduces less numerical diffusion. This is also the reason why the pressure variation is much better captured using OSS that ASGS, as it is seen from the pressure section at the wall $x = 3$. A similar behavior was found in the numerical examples presented in [15] for advection–diffusion and Stokes problems.

Referring to the cost of the calculation, it obviously depends on the particular implementation adopted. We have used as iterative solver the GMRES method only with diagonal scaling, with a Krylov dimension of 25 and a residual tolerance of 10^{-8}. Giving the reference 100 time units (t.u.) to the solution of the linear system for the ASGS method, the solution of the linear system for OSS has been 97.2 t.u., in spite of the fact that Jacobi iterations have been needed to deal with M^{-1}, as explained in Section 2.3. This reduction is due to the fact that 142 iterations have been required for ASGS and only 129 for OSS. The construction of the system matrix has taken 53.7 t.u. for OSS and 58.5 t.u. for ASGS.

4.2. Convergence test

The purpose of this test is to show that when the solution is smooth, the OSS method has an optimal convergence rate, similar to that of the ASGS formulation.

We take Ω as the unit square and the force term so that the exact solution is $p = 0$ and $\boldsymbol{u}(x, y) = (f(x)g'(y), -f'(x)g(y))$, with $f(x) = x^2(1-x)^2$ and $g(y) = y^2(1-y)^2$. This velocity field vanishes on $\partial\Omega$. The viscosity has been taken $\nu = 0.001$ and the advection velocity $\boldsymbol{a} = (2, 3)$. We have used meshes with different element sizes h, which once normalized range form 0.1 to 0.025.

In Fig. 3 we have plotted the convergence of the velocities obtained with the OSS and the ASGS methods as the mesh is refined in the discrete ℓ^2 norm and for both the Q_1 (bilinear) and Q_2 (biquadratic) interpolations (with the same set of nodes in both cases). This error is defined as

Please cite this article in press as: R. Codina, Analysis of a stabilized finite element approximation of the Oseen equations using orthogonal subscales, Applied Numerical Mathematics (2007), doi:10.1016/j.apnum.2006.11.011

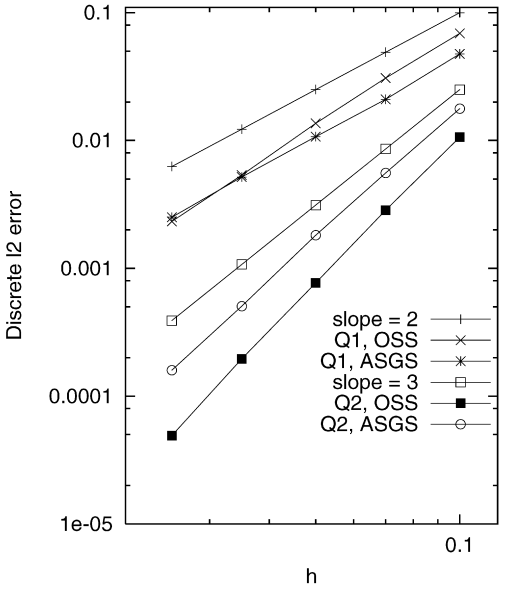

Fig. 3. Discrete ℓ^2 errors for Example 3 using Q_1 and Q_2 elements.

$$E = \left[\sum_{a=1}^{n_{\text{pts}}}\sum_{i=1}^{2}\left(\mathsf{U}_i^a - u_i(\boldsymbol{x}_a)\right)^2\right]^{1/2}\left[\sum_{a=1}^{n_{\text{pts}}}\sum_{i=1}^{2}\left(u_i(\boldsymbol{x}_a)\right)^2\right]^{-1/2},$$

where n_{pts} is the total number of nodal points, U_i^a is the ith component of the nodal velocity at node a and $\boldsymbol{x}_a$ are the coordinates of this node.

The optimal convergence rate that should be expected is 2 for Q_1 elements and 3 for the Q_2 case. From Fig. 3 it is seen that this is approximately what has been found. In both cases the convergence rate is slightly higher for the OSS method. These results are very similar to those obtained in [15] with the same test for the nonlinear Navier–Stokes equations.

5. Concluding remarks

Three different stabilized finite element formulations for the Oseen problem have been presented in this paper. Their main features are:

(1) The original method (referred to as method I in the paper) is directly based on the subgrid scale concept, assuming that the subscales are orthogonal to the finite element space. After some simple approximations, a stabilized formulation is obtained with two major benefits with respect to the original Galerkin method: it allows the use of equal velocity–pressure interpolations and it provides optimal control on the streamline derivative of the velocity field.
(2) The second method (method II) is somewhat simpler, since it introduces less coupling in the discrete velocity–pressure equations (although one more projection needs to be performed). Furthermore, stability and error estimates have been shown to hold in a norm finer than for method I, since now it is possible to control the orthogonal components of the convective term and the pressure gradient.
(3) If only the pressure interpolation is to be stabilized, a simplification of methods I and II has been proposed and analyzed. The norm in which stability and convergence have been proven depends explicitly on the mesh Reynolds number and the global Reynolds number.

Finally, the numerical experiments presented show that the OSS formulation is very accurate and introduces less numerical dissipation than the more usual ASGS method. This implies that it allows stronger localized oscillations near boundaries, but also that it leads to a sharper resolution of strong variations of the unknowns. This fact has as a

Please cite this article in press as: R. Codina, Analysis of a stabilized finite element approximation of the Oseen equations using orthogonal subscales, Applied Numerical Mathematics (2007), doi:10.1016/j.apnum.2006.11.011

consequence a better treatment of the pressure near boundaries. See [15,18] for further discussion about this point and some additional numerical results.

References

[1] M. Ainsworth, J.T. Oden, A Posteriori Error Estimation in Finite Element Analysis, Wiley–Interscience, New York, 2000.
[2] R. Becker, M. Braack, A finite element pressure gradient stabilization for the Stokes equations based on local projections, Calcolo 38 (2001) 173–199.
[3] J. Blasco, R. Codina, Space and time error estimates for a first order, pressure stabilized finite element method for the incompressible Navier–Stokes equations, Applied Numerical Mathematics 38 (2001) 475–497.
[4] P. Bochev, Z. Cai, T.A. Manteuffel, S.F. McCormick, Analysis of velocity–flux first-order system least-squares principles for the Navier–Stokes equations: Part I, SIAM Journal on Numerical Analysis 35 (1998) 990–1009.
[5] S.C. Brenner, L.R. Scott, The Mathematical Theory of Finite Element Methods, Springer, Berlin, 1994.
[6] F. Brezzi, J. Douglas, Stabilized mixed methods for the Stokes problem, Numerische Mathematik 53 (1988) 225–235.
[7] F. Brezzi, M. Fortin, Mixed and Hybrid Finite Element Methods, Springer, Berlin, 1991.
[8] F. Brezzi, M. Fortin, A minimal stabilisation procedure for mixed finite element methods, Numerische Mathematik 89 (2001) 457–491.
[9] F. Brezzi, L.P. Franca, T.J.R. Hughes, A. Russo, $b = \int g$, Computer Methods in Applied Mechanics and Engineering 145 (1997) 329–339.
[10] F. Brezzi, J. Pitkäranta, On the stabilization of finite element approximation of the Stokes problem, in: W. Hackbush (Ed.), Efficient Solution of Elliptic Systems, Vieweg, Braunschweig, 1984, pp. 11–19.
[11] F. Brezzi, J. Rappaz, P.A. Raviart, Finite dimensional approximation of nonlinear problems. Part I: Branches of non-singular solutions, Numerische Mathematik 36 (1981) 1–25.
[12] A.N. Brooks, T.J.R. Hughes, Streamline upwind/Petrov–Galerkin formulations for convection dominated flows with particular emphasis on the incompressible Navier–Stokes equation, Computer Methods in Applied Mechanics and Engineering 32 (1982) 199–259.
[13] E. Burman, P. Hansbo, Edge stabilization for Galerkin approximations of convection–diffusion–reaction problems, Computer Methods in Applied Mechanics and Engineering 193 (2004) 1437–1453.
[14] T. Chacón, A term by term stabilization algorithm for the finite element solution of incompressible flow problems, Numerische Mathematik 79 (1998) 283–319.
[15] R. Codina, Stabilization of incompressibility and convection through orthogonal sub-scales in finite element methods, Computer Methods in Applied Mechanics and Engineering 190 (2000) 1579–1599.
[16] R. Codina, A stabilized finite element method for generalized stationary incompressible flows, Computer Methods in Applied Mechanics and Engineering 190 (2001) 2681–2706.
[17] R. Codina, Stabilized finite element approximation of transient incompressible flows using orthogonal subscales, Computer Methods in Applied Mechanics and Engineering 191 (2002) 4295–4321.
[18] R. Codina, J. Blasco, A finite element formulation for the Stokes problem allowing equal velocity–pressure interpolation, Computer Methods in Applied Mechanics and Engineering 143 (1997) 373–391.
[19] R. Codina, J. Blasco, Analysis of a pressure-stabilized finite element approximation of the stationary Navier–Stokes equations, Numerische Mathematik 87 (2000) 59–81.
[20] J. Douglas, J. Wang, An absolutely stabilized finite element method for the Stokes problem, Mathematics of Computation 52 (1989) 495–508.
[21] L. Franca, T.J.R. Hughes, A.F.D. Loula, I. Miranda, A new family of stable elements for nearly incompressible elasticity based on a mixed Petrov–Galerkin finite element formulation, Numerische Mathematik 53 (1988) 123–141.
[22] L. Franca, R. Stenberg, Error analysis of some Galerkin least-squares methods for the elasticity equations, SIAM Journal on Numerical Analysis 28 (1991) 1680–1697.
[23] L.P. Franca, S.L. Frey, Stabilized finite element methods: II. The incompressible Navier–Stokes equations, Computer Methods in Applied Mechanics and Engineering 99 (1992) 209–233.
[24] V. Girault, P.A. Raviart, Finite Element Methods for Navier–Stokes Equations, Springer, Berlin, 1986.
[25] P.M. Gresho, On the theory of semi-implicit projection methods for viscous incompressible flow and its implementation via a finite element method that also introduces a nearly consistent mass matrix. Part I: Theory, International Journal for Numerical Methods in Fluids 11 (1990) 587–620.
[26] T.J.R. Hughes, Multiscale phenomena: Green's function, the Dirichlet-to-Neumann formulation, subgrid scale models, bubbles and the origins of stabilized formulations, Computer Methods in Applied Mechanics and Engineering 127 (1995) 387–401.
[27] T.J.R. Hughes, G.R. Feijóo, L. Mazzei, J.B. Quincy, The variational multiscale method—a paradigm for computational mechanics, Computer Methods in Applied Mechanics and Engineering 166 (1998) 3–24.
[28] T.J.R. Hughes, L.P. Franca, M. Balestra, A new finite element formulation for computational fluid dynamics: V. Circumventing the Babuška–Brezzi condition: a stable Petrov–Galerkin formulation for the Stokes problem accommodating equal-order interpolations, Computer Methods in Applied Mechanics and Engineering 59 (1986) 85–99.
[29] L. Tobiska, G. Lube, A modified streamline-diffusion method for solving the stationary Navier–Stokes equations, Numerische Mathematik 59 (1991) 13–29.
[30] L. Tobiska, R. Verfürth, Analysis of a streamline diffusion finite element method for the Stokes and Navier–Stokes equations, SIAM Journal on Numerical Analysis 33 (1996) 107–127.

Please cite this article in press as: R. Codina, Analysis of a stabilized finite element approximation of the Oseen equations using orthogonal subscales, Applied Numerical Mathematics (2007), doi:10.1016/j.apnum.2006.11.011